



DOE Award No.: DE-FE0023919

Quarterly Research Performance Progress Report

(Period Ending 10/31/20)

Deepwater Methane Hydrate Characterization & Scientific Assessment

Project Period 4: 10/01/19 - 09/30/20

Submitted by:

Peter B. Flemings

A handwritten signature in black ink that reads 'Peter B. Flemings'. The signature is written in a cursive style and is positioned above a horizontal line.

Signature

The University of Texas at Austin  
DUNS #: 170230239  
101 East 27<sup>th</sup> Street, Suite 4.300  
Austin, TX 78712-1500  
Email: [pflemings@jsg.utexas.edu](mailto:pflemings@jsg.utexas.edu)  
Phone number: (512) 475-8738

Prepared for:

United States Department of Energy  
National Energy Technology Laboratory

October 30, 2020



U.S. DEPARTMENT OF  
**ENERGY**

**NATIONAL ENERGY  
TECHNOLOGY LABORATORY**

**Office of Fossil Energy**

## DISCLAIMER

This report was prepared as an account of work sponsored by an agency of the United States Government. Neither the United States Government nor any agency thereof, nor any of their employees, makes any warranty, express or implied, or assumes any legal liability or responsibility for the accuracy, completeness, or usefulness of any information, apparatus, product, or process disclosed, or represents that its use would not infringe privately owned rights. Reference herein to any specific commercial product, process, or service by trade name, trademark, manufacturer, or otherwise does not necessarily constitute or imply its endorsement, recommendation, or favoring by the United States Government or any agency thereof. The views and opinions of authors expressed herein do not necessarily state or reflect those of the United States Government or any agency thereof.

# 1 ACCOMPLISHMENTS

This report outlines the progress of the second quarter of the sixth fiscal year of the project (Budget Period 4, Year 1). Highlights from this period include:

- **AAPG Volume 1 Publication:** A special volume of the AAPG Bulletin was published in September 2020, dedicated the initial results from the UT-GOM2-1 expedition. Six papers summarize the initial results of the expedition. This is part 1 of a multi-volume commitment by AAPG to this project. It is an exciting demonstration of the project's achievements. The links to the papers are provided below:

AAPG Bulletin, Vol. 104, No. 9, *Gas Hydrates in Green Canyon 955, Deep-water Gulf of Mexico: Part 1*

1. <http://dx.doi.org/10.1306/01062019165>
  2. <http://dx.doi.org/10.1306/05212019052>
  3. <http://dx.doi.org/10.1306/05212019027>
  4. <http://dx.doi.org/10.1306/01062018280>
  5. <http://dx.doi.org/10.1306/10151818125>
  6. <http://dx.doi.org/10.1306/04251918177>
  7. <http://dx.doi.org/10.1306/02262019036>
- **AAPG ACE Presentations:** The AAPG Annual Convention and Exhibition (ACE), held Sep 29 – Oct 1, included a dedicated session on gas hydrates systems. Six out of nine presentations for this session (*Theme 9: Analysis of Gas Hydrates Systems, I and II*) were presented by members of the project team (UT, UNH) and dedicated to UT-GOM2-1 science results.
  - **UT-GOM2-2 Shallow Hazard Assessments:** UT and Ohio State, after extensive geological and geophysical evaluation, completed a Shallow Hazard Assessment report for each proposed UT-GOM2-2 drilling location, pursuant to 30 CFR 250.214(f) and 250.244 (f). The Shallow Hazard Reports will accompany the UT-GOM2-2 Exploration Plan that is submitted to BOEM, and completes the geological and geophysical analysis for UT-GOM2-2 permitting efforts.
  - **PCTB Continued Testing:** Geotek has continued to test the PCTB at their test facility in Salt Lake City, Utah. The failure mode encountered during the PCTB Land Test II has been reproduced and is due to ingress of detritus and grit into the seal-carrier and ball-follower, jamming the ball valve. Geotek has incrementally designed and tested 9 modifications to address this observed failure mode. The modifications are currently being tested. Preliminary results show significant improvement.

## 1.1 Major Project Goals

The primary objective of this project is to gain insight into the nature, formation, occurrence and physical properties of methane hydrate-bearing sediments for the purpose of methane hydrate resource appraisal. This will be accomplished through the planning and execution of a state-of-the-art drilling, coring, logging, testing and analytical program that assess the geologic occurrence, regional context, and characteristics of marine methane hydrate deposits in the Gulf of Mexico Continental Shelf. Project Milestones are listed in Table 1-1, Table 1-2, and Table 1-3.

Table 1-1: Previous Milestones

Budget Period	Milestone	Milestone Description	Estimated Completion	Actual Completion	Verification Method
1	M1A	Project Management Plan	Mar-15	Mar-15	Project Management Plan
	M1B	Project Kick-off Meeting	Jan-15	Dec-14	Presentation
	M1C	Site Location and Ranking Report	Sep-15	Sep-15	Phase 1 Report
	M1D	Preliminary Field Program Operational Plan Report	Sep-15	Sep-15	Phase 1 Report
	M1E	Updated CPP Proposal Submitted	May-15	Oct-15	Phase 1 Report
	M1F	Demonstration of a Viable Pressure Coring Tool: Lab Test	Sep-15	Sep-15	Phase 1 Report
2	M2A	Document Results of BP1/Phase 1 Activities	Dec-15	Jan-16	Phase 1 Report
	M2B	Complete Updated CPP Proposal Submitted	Nov-15	Nov-15	QRPPR
	M2C	Scheduling of Hydrate Drilling Leg by IODP	May-16	May-17	Report directly to DOE PM
	M2D	Demonstration of a Viable Pressure Coring Tool: Land Test	Dec-15	Dec-15	PCTB Land Test Report, in QRPPR
	M2E	Demonstration of a Viable Pressure Coring Tool: Marine Test	Jan-17	May-17	QRPPR
	M2F	Update UT-GOM2-2 Operational Plan	Feb-18	Apr-18	Phase 2 Report
3	M3A	Document results of BP2 Activities	Apr-18	Apr-18	Phase 2 Report
	M3B	Update UT-GOM2-2 Operational Plan	Sep-19	Jan-19	Phase 3 Report

Table 1-2: Current Milestones

Budget Period	Milestone	Milestone Description	Estimated Completion	Actual Completion	Verification Method
4	M4A	Document results of BP3 Activities	Jan-20	Apr-20	Phase 3 Report
	M4B	Demonstration of a Viable Pressure Coring Tool: Lab Test	Feb-20	Jan-20	PCTB Lab Test Report, in QRPPR
	M4C	Demonstration of a Viable Pressure Coring Tool: Land Test	Mar-20	Mar-20	PCTB Land Test Report, in QRPPR

Table 1-3: Future Milestones

Budget Period	Milestone	Milestone Description	Estimated Completion	Actual Completion	Verification Method
5	M5A	Document Results of BP4 Activities	Dec-20	-	Phase 4 Report
	M5B	Complete Contracting of UT-GOM2-2 with Drilling Vessel	May-21	-	QRPPR
	M5C	Complete Project Sample and Data Distribution Plan	Jul-22	-	Report directly to DOE PM
	M5D	Complete Pre-Expedition Permitting Requirements for UT-GOM2-2	Dec-21	-	QRPPR
	M5E	Complete UT-GOM2-2 Operational Plan Report	May-21	-	QRPPR
	M5F	Complete UT-GOM2-2 Field Operations	Jul-22	-	QRPPR
6	M6A	Document Results of BP5 Activities	Dec-22	-	Phase 5 Report
	M6B	Complete Preliminary Expedition Summary	Dec-22	-	Report directly to DOE PM
	M6C	Initiate comprehensive Scientific Results Volume	Jun-23	-	Report directly to DOE PM
	M6D	Submit set of manuscripts for comprehensive Scientific Results Volume	Sep-24	-	Report directly to DOE PM

## 1.2 What Was Accomplishments Under These Goals

### 1.2.1 Previous Project Periods

Tasks accomplished in previous project periods (Phase 1, 2, and 3) are summarized in Table 1-4, Table 1-5, and Table 1-6.

Table 1-4: Tasks Accomplished in Phase 1

PHASE 1/BUDGET PERIOD 1	
<b>Task 1.0</b>	<b>Project Management and Planning</b>
<b>Task 2.0</b>	<b>Site Analysis and Selection</b>
Subtask 2.1	Site Analysis
Subtask 2.2	Site Ranking / Recommendation
<b>Task 3.0</b>	<b>Develop Operational Plan for UT-GOM2-2 Scientific Drilling Program</b>
<b>Task 4.0</b>	<b>Complete IODP Complimentary Project Proposal</b>
<b>Task 5.0</b>	<b>Pressure Coring and Core Analysis System Modifications and Testing</b>
Subtask 5.1	PCTB Scientific Planning Workshop
Subtask 5.2	PCTB Lab Test
Subtask 5.3	PCTB Land Test Prep

Table 1-5: Tasks Accomplished in Phase 2

PHASE 2/BUDGET PERIOD 2	
<b>Task 1.0</b>	<b>Project Management and Planning</b>
<b>Task 6.0</b>	<b>Technical and Operational Support of Complimentary Project Proposal</b>
<b>Task 7.0</b>	<b>Continued Pressure Coring and Core Analysis System Modifications and Testing</b>
Subtask 7.1	Review and Complete NEPA Requirements for PCTB Land Test
Subtask 7.2	PCTB Land Test
Subtask 7.3	PCTB Land Test Report
Subtask 7.4	PCTB Modification
<b>Task 8.0</b>	<b>UT-GOM2-1 Marine Field Test</b>
Subtask 8.1	Review and Complete NEPA Requirements for UT-GOM2-1
Subtask 8.2	UT-GOM2-1 Operational Plan
Subtask 8.3	UT-GOM2-1 Documentation and Permitting
Subtask 8.4	UT-GOM2-1 Marine Field Test of Pressure Coring System
Subtask 8.5	UT-GOM2-1 Marine Field Test Report
<b>Task 9.0</b>	<b>Develop Pressure Core Transport, Storage, and Manipulation Capability</b>
Subtask 9.1	Review and Complete NEPA Requirements for Core Storage and Manipulation
Subtask 9.2	Hydrate Core Transport
Subtask 9.3	Storage of Hydrate Pressure Cores
Subtask 9.4	Refrigerated Container for Storage of Hydrate Pressure Cores

<i>Subtask 9.5</i>	<i>Hydrate Core Manipulator and Cutter Tool</i>
<i>Subtask 9.6</i>	<i>Hydrate Core Effective Stress Chamber</i>
<i>Subtask 9.7</i>	<i>Hydrate Core Depressurization Chamber</i>
<b>Task 10.0</b>	<b>Core Analysis</b>
<i>Subtask 10.1</i>	<i>Routine Core Analysis (UT-GOM2-1)</i>
<i>Subtask 10.2</i>	<i>Pressure Core Analysis (UT-GOM2-1)</i>
<i>Subtask 10.3</i>	<i>Hydrate Core-Log-Seismic Synthesis (UT-GOM2-1)</i>
<b>Task 11.0</b>	<b>Update Operational Plan for UT-GOM2-2 Scientific Drilling Program</b>
<b>Task 12.0</b>	<b>UT-GOM2-2 Scientific Drilling Program Vessel Access</b>

Table 1-6: Tasks Accomplished in Phase 3

<b>PHASE 3/BUDGET PERIOD 3</b>	
<b>Task 1.0</b>	<b>Project Management and Planning</b>
<b>Task 6.0</b>	<b>Technical and Operational Support of CPP Proposal</b>
<b>Task 9.0</b>	<b>Develop Pressure Core Transport, Storage, and Manipulation Capability</b>
<i>Subtask 9.8</i>	<i>X-ray Computed Tomography</i>
<i>Subtask 9.9</i>	<i>Pre-Consolidation System</i>
<b>Task 10.0</b>	<b>Core Analysis</b>
<i>Subtask 10.4</i>	<i>Continued Pressure Core Analysis (UT-GOM2-1)</i>
<i>Subtask 10.5</i>	<i>Continued Hydrate Core-Log-Seismic Synthesis (UT-GOM2-1)</i>
<i>Subtask 10.6</i>	<i>Additional Core Analysis Capabilities</i>
<b>Task 11.0</b>	<b>Update Operational Plan for UT-GOM2-2 Scientific Drilling Program</b>
<b>Task 12.0</b>	<b>UT-GOM2-2 Scientific Drilling Program Vessel Access</b>
<b>Task 13.0</b>	<b>Maintenance and Refinement of Pressure Core Transport, Storage, and Manipulation Capability</b>
<i>Subtask 13.1</i>	<i>Hydrate Core Manipulator and Cutter Tool</i>
<i>Subtask 13.2</i>	<i>Hydrate Core Effective Stress Chamber</i>
<i>Subtask 13.3</i>	<i>Hydrate Core Depressurization Chamber</i>
<i>Subtask 13.4</i>	<i>Develop Hydrate Core Transport Capability for UT-GOM2-2 Scientific Drilling Program</i>
<i>Subtask 13.5</i>	<i>Expansion of Pressure Core Storage Capability for UT-GOM2-2 Scientific Drilling Program</i>
<i>Subtask 13.6</i>	<i>Continued Storage of Hydrate Cores from UT-GOM2-1</i>
<b>Task 14.0</b>	<b>Performance Assessment, Modifications, and Testing of PCTB</b>
<i>Subtask 14.1</i>	<i>PCTB Lab Test</i>
<i>Subtask 14.2</i>	<i>PCTB Modifications/Upgrades</i>
<b>Task 15.0</b>	<b>UT-GOM2-2 Scientific Drilling Program Preparations</b>
<i>Subtask 15.1</i>	<i>Assemble and Contract Pressure Coring Team Leads for UT-GOM2-2 Scientific Drilling Program</i>
<i>Subtask 15.2</i>	<i>Contract Project Scientists and Establish Project Science Team for UT-GOM2-2 Scientific Drilling Program</i>

## 1.2.2 Current Project Period

Current project period tasks are shown in Table 1-7.

Table 1-7: Current Project Tasks

<b>PHASE 4/BUDGET PERIOD 4</b>	
<b>Task 1.0</b>	<b>Project Management and Planning</b>
<b>Task 10.0</b>	<b>Core Analysis</b>
<i>Subtask 10.4</i>	<i>Continued Pressure Core Analysis (GOM2-1)</i>
<i>Subtask 10.5</i>	<i>Continued Hydrate Core-Log-Seismic Synthesis (UT-GOM2-1)</i>
<i>Subtask 10.6</i>	<i>Additional Core Analysis Capabilities</i>
<i>Subtask 10.7</i>	<i>Hydrate Modeling</i>
<b>Task 11.0</b>	<b>Update Operational Plan for UT-GOM2-2 Scientific Drilling Program</b>
<b>Task 12.0</b>	<b>UT-GOM2-2 Scientific Drilling Program Vessel Access</b>
<b>Task 13.0</b>	<b>Maintenance and Refinement of Pressure Core Transport, Storage, and Manipulation Capability</b>
<i>Subtask 13.1</i>	<i>Hydrate Core Manipulator and Cutter Tool</i>
<i>Subtask 13.2</i>	<i>Hydrate Core Effective Stress Chamber</i>
<i>Subtask 13.3</i>	<i>Hydrate Core Depressurization Chamber</i>
<i>Subtask 13.4</i>	<i>Develop Hydrate Core Transport Capability for UT-GOM2-2 Scientific Drilling Program</i>
<i>Subtask 13.5</i>	<i>Expansion of Pressure Core Storage Capability for UT-GOM2-2 Scientific Drilling Program</i>
<i>Subtask 13.6</i>	<i>Continued Storage of Hydrate Cores from UT-GOM2-1</i>
<i>Subtask 13.7</i>	<i>X-ray Computed Tomography</i>
<i>Subtask 13.8</i>	<i>Pre-Consolidation System</i>
<b>Task 14.0</b>	<b>Performance Assessment, Modifications, and Testing of PCTB</b>
<i>Subtask 14.1</i>	<i>PCTB Lab Test</i>
<i>Subtask 14.2</i>	<i>PCTB Modifications/Upgrades</i>
<i>Subtask 14.3</i>	<i>PCTB Land Test</i>
<b>Task 15.0</b>	<b>UT-GOM2-2 Scientific Drilling Program Preparations</b>
<i>Subtask 15.3</i>	<i>Permitting for UT-GOM2-2 Scientific Drilling Program</i>

### 1.2.2.1 Task 1.0 – Project Management & Planning

Status: Ongoing

#### 1. Coordinate the overall scientific progress, administration and finances of the project:

- Monitored and controlled project scope, costs, and schedule.
- Continued to support the Budget Period 4 (BP4) to Budget Period 5 (BP5) budget period transition:
  - The BP4-BP5 continuation application submitted by UT in the previous quarter was approved by DOE in August, 2020.
  - The BP4-BP5 budget period transition occurs on Oct 1, 2020.
- Successfully interviewed and hired four new project team members:
  - Post-doctoral researcher
  - Research Associate
  - Research and Engineering/Science Associate
  - Graduate Student

#### 2. Communicated with project team and sponsors:

- Organized and coordinated project team and stakeholder meetings.
- Organized task-specific team working meetings to plan and execute project tasks (e.g. PCTB development, PCTB development, UT-GOM2-2 operations planning, UT-GOM2-2 science and sample distribution planning, UT-GOM2-2 permitting, and UT-GOM2-2 vessel selection.).
- Organized sponsor meetings.
- Managed SharePoint sites, email lists, and archive/website.

#### 3. Coordinated and supervised subcontractors and service agreements:

- Actively managed subcontractors.
- Monitored schedules and ensured that contractual obligations were met.
- Amended all subcontract agreements to include the new foreign national language.
- Amended all subcontract agreements to fund Year 1 of BP5.

## 1.2.2.2 Task 10.0 – Core Analysis

Status: Ongoing

### 1.2.2.2.1 Subtask 10.4 – Continued Pressure Core Analysis

#### A. Pressurized Core Analysis

##### A1. Quantitative Degassing

- UT performed two quantitative degassing experiments in July 2020: H005-07FB-3, 49-66 cm and H005-2FB2, 5-32 cm. Both of these samples contained multiple lithofacies and were used to collect bulk gas samples for molecular hydrocarbon, bulk methane C and H isotope, and noble gas composition. Gases were collected using an inflatable bag as shown in Figure 1-1.



Figure 1-1: Image of inflatable bag attached to the quantitative degassing manifold used in order to capture 100% of the gas produced from the dissociation of hydrate-bearing sediment from UT-GOM2-1. Samples taken from the bag will be used to measure the bulk chemical ratios of the dissociated gases.

##### A2. Permeability measurement of pressure core

- UT continued measuring the permeability of UT-GOM2-1 pressure cores. During this quarter, we cut one pressure core section from UT-GOM2-1-H005-2FB-2. We completed the measurement of effective permeability of 2FB-2 core (2FB-2-01) with brine.
- We found that the effective permeability of core 2FB-2-01, in comparison to other core samples, does not decrease with increasing effective stress. At in situ stress, the effective permeability is about 2 mD for 2FB-2-01 (Figure 1-2).

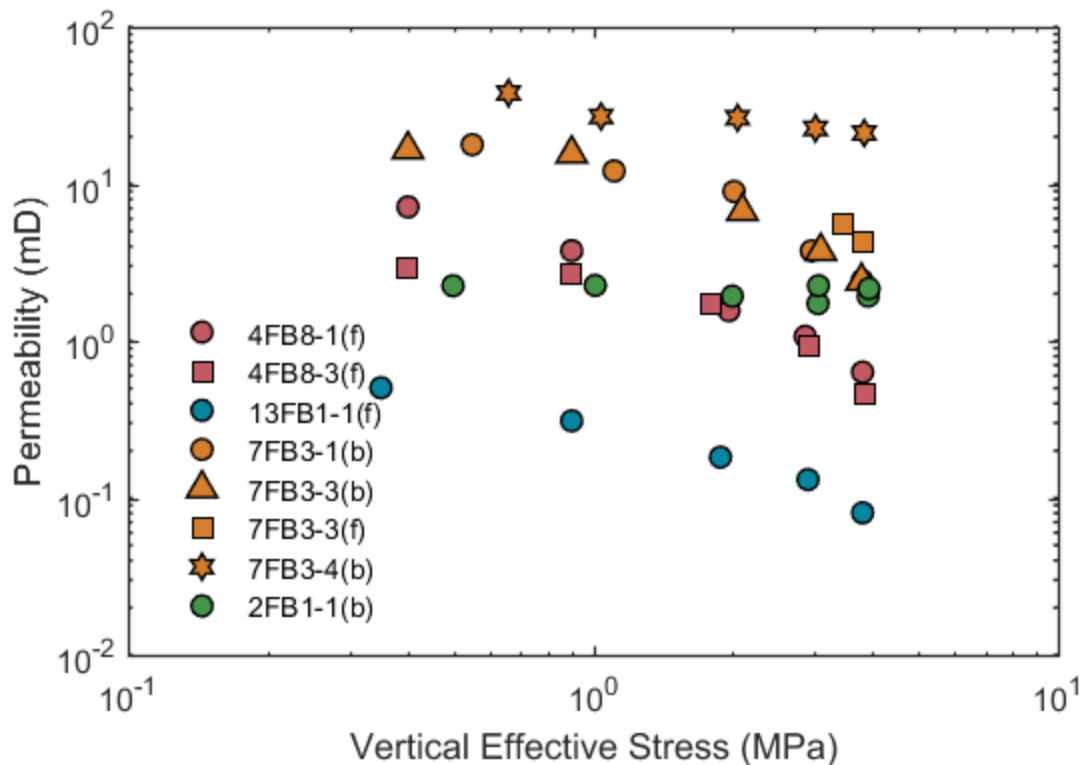


Figure 1-2: A summary of effective permeabilities of UT-GOM2-1 hydrate bearing sandy silt sediment from pressure core sections as a function of vertical effective stress. Legend note: b-measured by brine (salinity = 3.5%), f-measured by freshwater (salinity = 0). During the test, the pore fluid pressure is 24.8 MPa and temperature is 6.5 °C.

## B. Depressurized Pressure Core Analysis

- UNH continues to work on synthesizing the grain size, CHNS, and sediment composition data to document the sediment transport regimes throughout the reservoir and subsequent early diagenesis of the GC-955 hydrate-bearing sediments. Figure 1-3 shows the sorting of all Bulk and Organic Carbon-Free GOM2-1 samples measured to date plotted against their median grain size by laser diffraction. Smaller sorting values equate to better sorting while smaller Phi values equate to larger grain sizes. The UNH lab standard, Wallis Beach Sand, a natural beach sand, is also shown for reference. Sorting was calculated by the Folk and Ward (1957) sorting equation. All the measurements document a silt dominated reservoir, with three distinct sediment facies defined by their grain size distributions and sorting characteristics: Type C samples are the coarsest samples but have variable sorting that is consistent with turbidite deposition from variable energy turbidity currents. Type B and Type A samples are finer grained and less sorted, characteristic of fine grained deposition during the waning energy of turbidity currents and lower energy hemipelagic settling between turbidity current events. The increased sorting of all samples after organic carbon removal, reflects the variable size of organic carbon deposited during and between turbidity current events and documents that both the turbidites and intervening clays contain measurable organic carbon. In terms of textural classification, Type A samples

range from silty clays to clayey silts, Type B samples are clayey silts, and Type C samples range from silty sand to sandy silt.

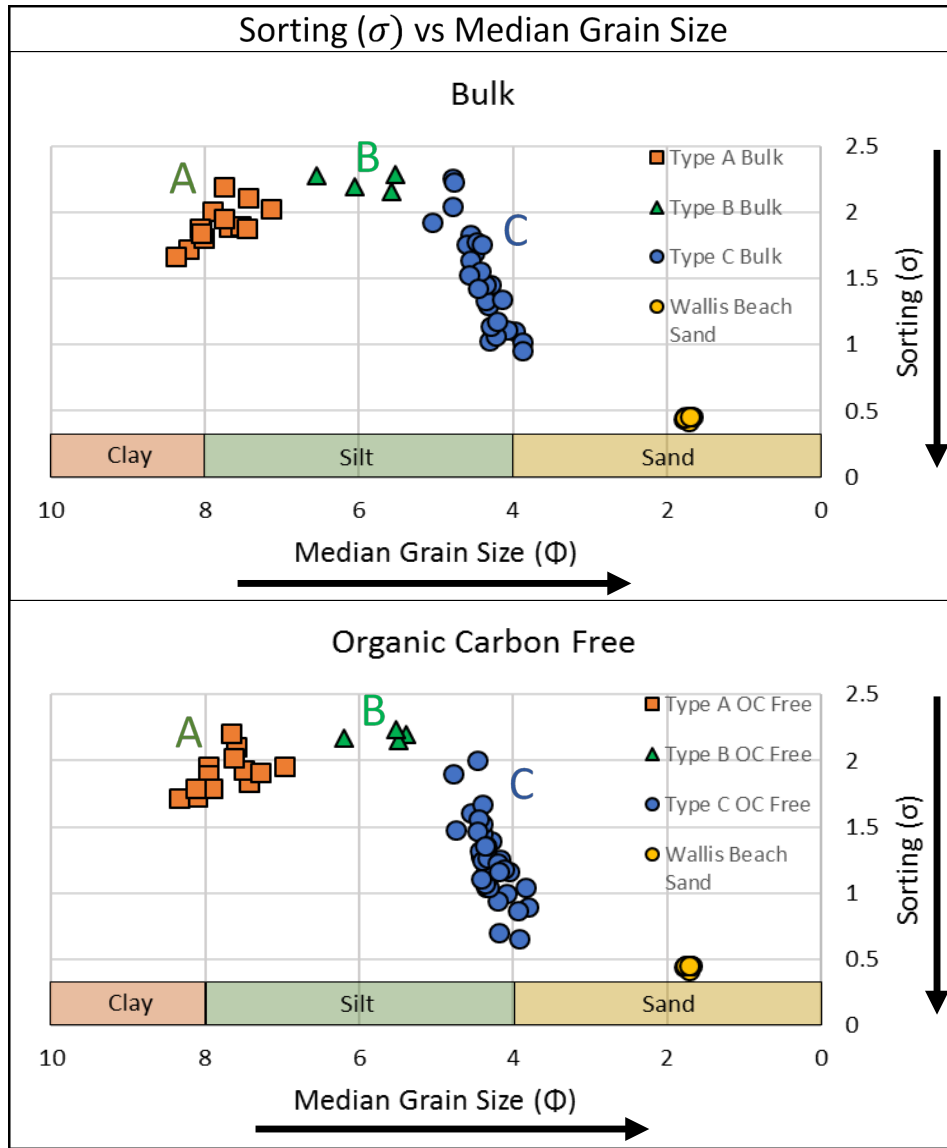


Figure 1-3: Sorting of all Bulk and Organic Carbon-Free GOM2-1 samples plotted against their median grain size (Phi units) from measurements of grain size completed at UNH using laser diffraction. Smaller sorting values equate to better sorting while smaller Phi values equate to larger grain sizes. The UNH lab standard, Wallis Beach Sand, a natural beach sand, is also shown for reference. Sorting was calculated by the Folk and Ward (1957) sorting equation.

#### 1.2.2.2.2 Subtask 10.5 – Continued Hydrate Core-Log-Seismic Synthesis

- No update this period.

#### 1.2.2.2.3 Subtask 10.6 – Additional Analysis Capabilities

- UNH received new equipment for assessing the total organic carbon content of sediments (TOC). UT-GOM2-1 TOC measurements will be repeated to confirm the TOC content measured using the old equipment before it was destroyed from a water leak.

#### 1.2.2.2.4 Subtask 10.7 – Hydrate Modeling

- No update this period.

#### 1.2.2.2.5 Other – Publications

- The first special issue of the AAPG Bulletin dedicated to UT-GOM2-1, GC 955 (Figure 1-4) was published. See AAPG Bulletin, Issue 104, 9, September 2020. *Gas Hydrates in Green Canyon 955, Deep-water Gulf of*

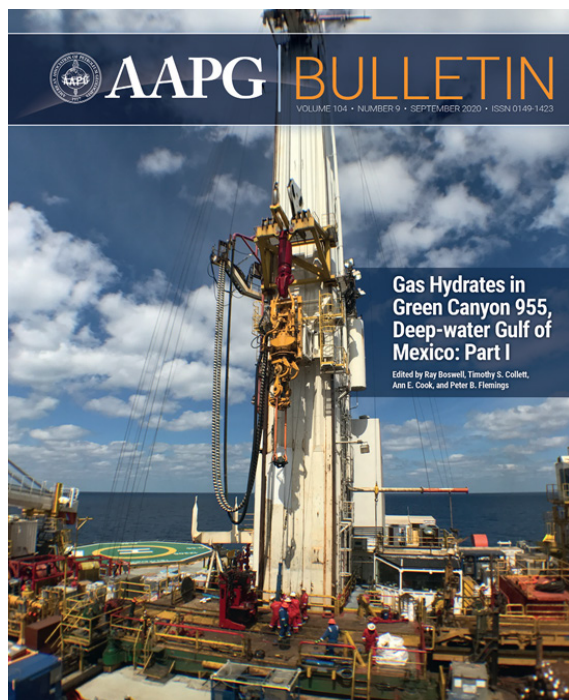


Figure 1-4: AAPG Bulletin, Vol. 104 Number 9, Sept 2020

*Mexico: Part 1.* Publications include:

1. Boswell, R., Collet, T.C., Cook, A.E., Flemings, P.B., 2020, Introduction to Special Issue: Gas Hydrates in Green Canyon Block 955, deep-water Gulf of Mexico: Part I: AAPG Bulletin, v. 104, no. 9, p. 1844-1846, <http://dx.doi.org/10.1306/bltnintro062320>.
2. Flemings, P. B., S. C. Phillips, R. Boswell, T. S. Collett, A. E. Cook, T. Dong, and M. Frye, et al., 2020, Pressure coring a Gulf of Mexico deep-water turbidite gas hydrate reservoir: Initial results from The University of Texas-Gulf of Mexico 2-1 (UT-GOM2-1) Hydrate Pressure Coring Expedition: AAPG Bulletin, v. 104, no. 9, p. 1847-1876, <http://dx.doi.org/10.1306/05212019052>.
3. Thomas, C., S. C. Phillips, P. B. Flemings, M. Santra, H. Hammon, T. S. Collett, and A. Cook, et al., 2020, Pressure-coring operations during The University of Texas-Gulf of Mexico 2-1 (UT-GOM2-1) Hydrate Pressure Coring Expedition in Green Canyon Block 955, northern Gulf of Mexico: AAPG Bulletin, v. 104, no. 9, p. 1877–1901, <http://dx.doi.org/10.1306/02262019036>.
4. Portnov, A., A. E. Cook, M. Heidari, D. E. Sawyer, M. Santra, and M. Nikolidakou, 2020, Salt-driven evolution of a gas hydrate reservoir in Green Canyon, Gulf of Mexico: AAPG Bulletin, v. 104, no. 9, p. 1903–1919, <http://dx.doi.org/10.1306/10151818125>.
5. Santra, M., P. B. Flemings, E. Scott, and P. K. Meazell, 2020, Evolution of gas hydrate-bearing deep-water channel-levee system in abyssal Gulf of Mexico: Levee growth and deformation: AAPG Bulletin, v. 104, no. 9, p. 1921–1944, <http://dx.doi.org/10.1306/04251918177>

6. Meazell, K., P. Flemings, M. Santra, and J. E. Johnson, 2020, Sedimentology and stratigraphy of a deep-water gas hydrate reservoir in the northern Gulf of Mexico: AAPG Bulletin, v. 104, no. 9, p. 1945–1969, <http://dx.doi.org/10.1306/05212019027>.
  7. Phillips, S. C., P. B. Flemings, M. E. Holland, P. J. Schultheiss, W. F. Waite, J. Jan, E. G. Petrou, and H. Hammon, 2020, High concentration methane hydrate in a silt reservoir from the deep-water Gulf of Mexico: AAPG Bulletin, v. 104, no. 9, p. 1971–1995, <http://dx.doi.org/10.1306/01062018280>.
  8. Fang, Y., P. B. Flemings, H. Daigle, S. C. Phillips, P. K. Meazell, and K. You, 2020, Petrophysical properties of the Green Canyon Block 955 hydrate reservoir inferred from reconstituted sediments: Implications for hydrate formation and production: AAPG Bulletin, v. 104, no. 9, p. 1997–2028, <http://dx.doi.org/10.1306/01062019165>.
- Ohio State published a new paper on our gas geochemistry sampling technique:
    1. Moore, M., Phillips, S., Cook, A.E. and Darrah, T., (2020, in review) Improved sampling technique to collect natural gas from hydrate-bearing pressure cores. Applied Geochemistry, Volume 122, November 2020, p. 104773, <https://doi.org/10.1016/j.apgeochem.2020.104773>.
  - UT with UNH prepared five presentations for the AAPG virtual Conference, Oct 1, Theme 9: Analysis of Natural Gas Hydrate Systems I & II
    1. Kehua You, *Impact of Coupled Free Gas Flow and Microbial Methanogenesis on the Formation and Evolution of Concentrated Hydrate Deposits*
    2. Peter Flemings, *Pressure Coring a Gulf of Mexico Deep-Water Turbidite Gas Hydrate Reservoir: The UT-GOM2-1 Hydrate Pressure Coring Expedition*
    3. Stephen Phillips, *High Concentration Methane Hydrate in a Silt Reservoir from the Deep-Water Gulf of Mexico*
    4. Joel Johnson, *Grain Size, TOC, and TS in Gas Hydrate Bearing Turbidite Facies at Green Canyon Site 955, Gulf of Mexico*
    5. Yi Fang, *Petrophysical Properties of Hydrate-Bearing Siltstone from UT-GOM2-1 Pressure Cores*
    6. Manasij Santra, *Gas Hydrate in a Fault-Compartmentalized Anticline and the Role of Seal, Green Canyon, Abyssal Northern Gulf of Mexico*
  - AAPG Editors continued working on the AAPG Volumes 2-3.
  - Ohio State has four AAPG papers in review
    1. Oti, E., Cook, A.E., Phillips, S., and Holland, M., (2020, accepted pending revisions) Using X-ray Computed Tomography (XCT) to Estimate Hydrate Saturation in Sediment Cores from Green Canyon 955, northern Gulf of Mexico. AAPG Bulletin. Accepted, Additional revisions were submitted this quarter.
    2. Moore, M., Phillips, S., Cook, A.E. and Darrah, T., (2020, in review) Microbial source of methane in hydrates from Green Canyon Block 955 in the Gulf of Mexico. Submitted this quarter. AAPG Bulletin. Revisions are currently in process.

3. Cook, A.E. and Portnov, A., (2020, in review) Chapter 5. Seismic detection of natural gas hydrate systems in Interpretation of seismic data in complex systems. Elsevier.
  4. Wei, L., Cook, A.E., You, K. (2020, in review). Methane Migration Mechanisms for the GC 955 Gas Hydrate Reservoir, Northern Gulf of Mexico. AAPG Bulletin.
- Oregon State has a paper in review
    1. *Impact of X-ray imaging on Biochemistry*, Frontiers in Microbiology
  - UT, Ohio State, UNH, UW, and Columbia all continued preparing UT-GOM2-1 Data Reports. Data Report archive experimental or observational data that is not captured in publications. The reports highlight methods and results but do not include any interpretation of the results.
    1. Data reports on high-resolution Leica imaging of sediments, X-ray diffraction, and seismic pre-stack waveform inversion were finalized and published. Published Data Reports can be found on [OSTI.gov](http://OSTI.gov) (search *UT-GOM2-1*), in the UT-GOM2-1 Expedition Proceedings (<https://ig.utexas.edu/energy/genesis-of-methane-hydrate-in-coarse-grained-systems/expedition-ut-gom2-1/reports/>) and in the UT-GOM2-1 Data Directory (<http://www-udc.ig.utexas.edu/gom2/>).

### 1.2.2.3 Task 11.0 – Update Operations Plan for UT-GOM2-2 Scientific Drilling Program

**Status:** Ongoing

#### Drilling Fluid

- A proposal for the use of salt-saturated, water-based drilling mud was submitted to UT as a consideration for UT-GOM2-1. The additional salt moves the hydrate stability boundary to close to our estimated coring conditions and does not give us enough room to operate. Figure 1-5 plots the in situ and expected borehole temperatures for WR313 (UT-GOM2-2) and GC 955 (UT-GOM2-1) against the hydrate stability boundary for different salinities (dashed lines). The distance between the estimated borehole temperature and the hydrate stability boundary for the salinity proposed (Figure 1-5, large light blue arrows) indicate how large of a temperature increase that can be tolerated before the pressure core might be compromised (degraded). The window for WR313 is smaller than the expected temperature rise as estimated from temperature swings measured at GC 955. More details can be found in **Attachment A**.

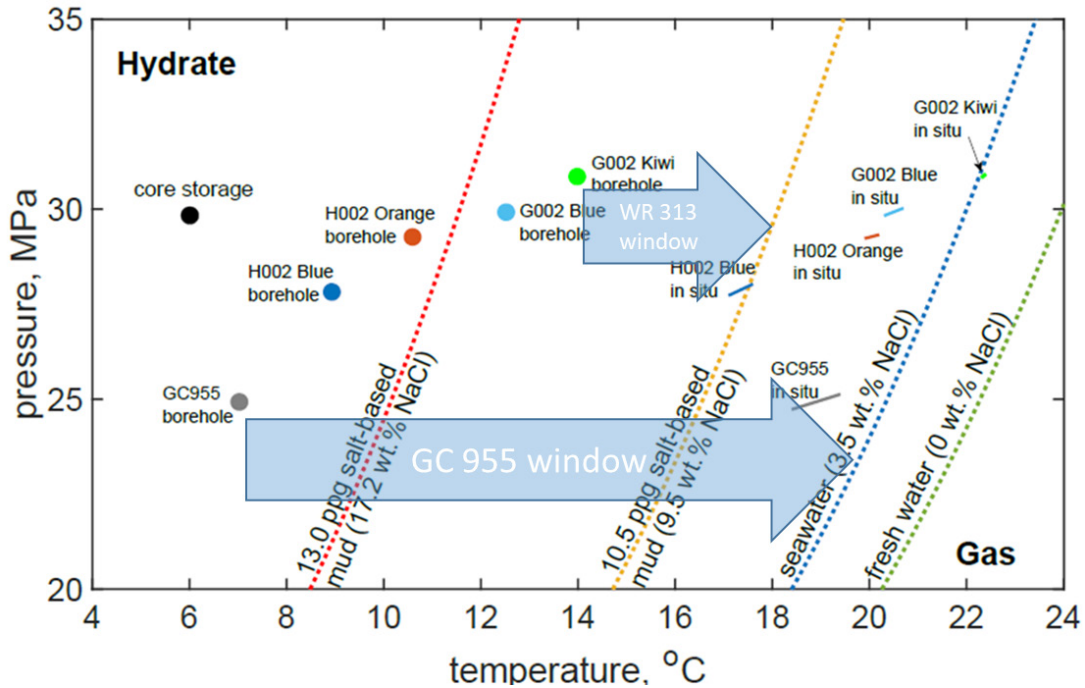


Figure 1-5: Methane hydrate phase diagram for different salinities. The dotted green, blue, orange and red lines are the methane hydrate phase boundaries for fresh water (0 wt.% NaCl), seawater (3.5 wt.% NaCl, the assumed in-situ salinity), 10.5 ppg salt-based mud (9.5 wt.% NaCl) and 13.0 ppg salt-based mud (17.2 wt.% NaCl), respectively. Methane hydrate is stable to the left of the phase boundary and unstable to the right. The solid light blue and orange lines are the in situ conditions for the H002 Blue and Orange sands, respectively. We used the temperature LWD borehole temperature to estimate the coring borehole temperature. The pressure gradient is 0.465 psi/ft. The solid dots are the estimated borehole temperatures and pressures while coring for each sand. The large blue arrows highlight the amount of temperature increase that can be tolerated as the core is brought from the bottom of the hole to the rig floor. The hydrate phase boundaries are calculated by the models presented in Liu and Flemings (2007). The black dot shows the expected pressure and temperature conditions for off-shore core storage of 6 oC (42.8 F) and 30 MPa (4351 psi).

### Pressure Core degradation

- An initial technical assessment of the degradation of pressure cores from UT-GOM2-1 during long term storage was started in order to determine any actions that might be taken prior to UT-GOM2-2 in order to better preserve the core.
  - Pressure cores are stored inside high pressure storage chambers with fresh water surrounding the core liner
  - Core degradation is assumed to be a result of methane dissociating from hydrate within the core and dissolving into the storage chamber fluid over long periods of time.
  - A methane mass balance calculation of an ideal core (40% porosity, 90% hydrate saturation, 111 cm long, homogeneous sandy silt) was used to estimate the amount of core degradation we might expect to see in pressure cores. The total volume of storage fluid that the core was approximately 1.3 L. The mass balance estimate predicted that 25 mL of hydrate (1.9% of the hydrate originally in the core) would dissociate and dissolve into the 1.3 L of storage fluid. Radial core loss was estimated from the volume of hydrate lost assuming the following assumptions:

- a homogeneous porosity of 40%,
- a hydrate saturation of 90%,
- a perfectly round core,
- hydrate is homogeneously lost along the outside of the core,
- and core sediment falls away from the core as the hydrate dissociates.

Thus, 25 mL of hydrate loss equates to the core radius shrinking by 0.15 mm homogeneously along the entire length of the core.

- Figure 1-6 shows an example of the degradation for core H005-05FB-3. Core degradation appears to be higher at the bottom of the core (the end that is open to the storage fluid and that faces up during storage).
- Core degradation was estimated from the images by comparing the core diameter for four different biscuits before and after storage (Figure 1-6, yellow boxes). The radial loss from each biscuit was determined to be 1.8 mm, 1.8 mm, 0.7 mm, and 0 mm, for biscuits 1 through 4, respectively, with a high margin of error. Using the assumptions above, this core radial loss equates to a hydrate volume loss of 34 mL. Thus, the estimate of the loss using a mass balance approach and from inspection of the core images is within a factor of two. Thus, we believe we can account for most of the core loss from exposure to fresh (0% salinity, 0% dissolved methane) storage fluid during longer periods of core storage.
- Additional work needs to be done to compare other cores. A wide range of examples was discussed at the Pressure Core working group meeting.

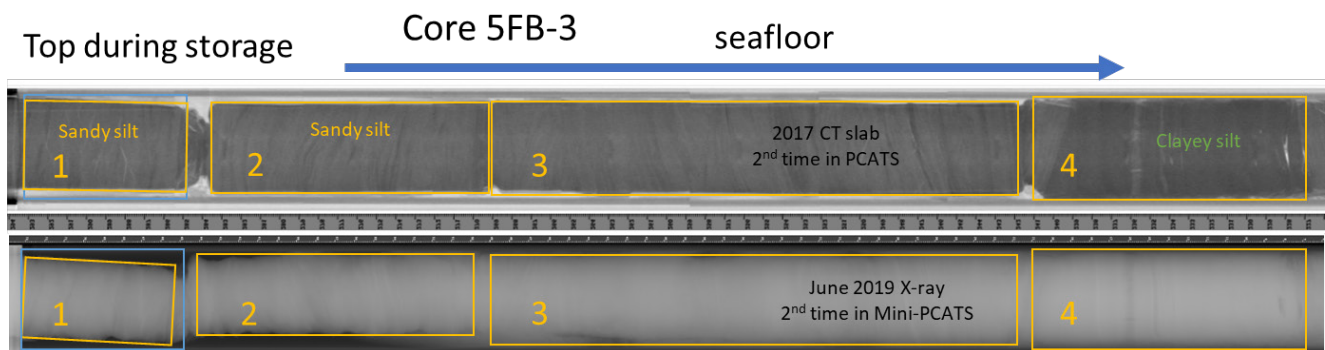


Figure 1-6: Images of the bottom 77 cm of core section H005-05FB-3 from before and after storage. Top image: CT 3D) cross section (slab section) of the bottom 77 cm of 5FB-3 taken using PCATS during the expedition in May of 2017. Lower density is bright and higher density is dark. Biscuits Interbedded layers of sandy silt and clayey silt are evident. Core outer edge is cleanly cut. Bottom most biscuit of sandy silt (far left) is slight smaller that higher up the core. Bottom image: X-ray (2D) image of the bottom 77 cm of 5FB-3 taken using Mini-PCATS after 2 years of storage in June of 2019 during which time the storage fluid was fully replace once. Higher density is bright and lower density is dark. The core edge after storage, especially at the very bottom (far left), is ratty and shrunken. Sediment appears to have fallen away and collected in the water between the core and the core liner. Clayey silt biscuit (far right) appears to have little to no radial loss. Yellow boxes show the biscuits and identified core diameter for each of four biscuits used to estimate core loss.

### UT-GOM2-1 Science and Sample Distribution plan

- Version 1 of the UT-GOM2-1 Science and Sample Distribution plan was released. The plan contains:
  - A review of the Science Objectives with rationale and specific plan to meet each objective (~15 pages)
  - The detailed Coring Plan including core points with LWD logs from JIP II
  - On-board and Dockside Pressure and Conventional Core analyses and sample allocation/movement
  - Required Equipment and Personnel
  - Appendix for Detailed methods and analytical descriptions
  - Appendix describing modification to a 4-well plan
  - Appendix describing modification to compensate for Cook APL
- A meeting was held to gather recommendations on the UT-GOM2-1 Science and Sample Distribution Plan from our Technical Advisory Group (TAG, members Ray Boswell, Tim Collett, Steve Phillips, Bill Waite, Yongkoo Seol, Sheng Dai, Peter Flemings, Carla Thomas). The following recommendations were captured and will be incorporated into the plan (Version 2):
  - Prioritize the allowance PC pair above the Blue sand (Blue sand seal) in H002. Great opportunity here for many aspects of the program.
  - Check in with Geotek on best shallow pressure coring technique – maybe operate PCTB like a push corer: low rotation, low flow rates
  - Make sure there is a component contrasting conventional vs pressure cores for microbiological research – opportunity to study the effect of pressure on microbiology
  - Check with Rick Colwell and others on the opportunity to collect samples from pressure cores using Geotek’s LN2 apparatus at the dock
  - All XRD samples should go to the same lab; include detailed clay analysis of all major units (in triplicate)- James Hutton Institute
  - All post-expedition laser particle size grain size measurements should be done at the same lab - UNH, settling method grain size measurements need to be done at UT
  - Make sure we have supplies and protocols in place for collecting gas hydrate samples from conventional core
  - Take vane shear measurements on the ends of cores on-board and at the dock

#### 1.2.2.4 Task 12.0 – UT-GOM2-2 Scientific Drilling Program Vessel Access

**Status:** Ongoing

- The Vessel Procurement Team held weekly meetings to work the issues of vessel selection and acquisition strategy.

- Evaluated costs/benefits of large rig vs small rig (e.g. day rates, vertical pipe racking, mud storage capacity, ROVs, deck space, etc.).
- Developed required inputs to the vessel requirements document:
  1. Time and resources estimates for the base cases, allowance cores, and contingency scenarios for both the 2-well and 4-well programs
  2. Requested draft volume estimates and quotes from MI SWACO based on drilling programs. Refined based on our institutional knowledge of coring in the GOM (e.g. JIP, GC-955)
- Updated vessel specifications based on current operational and science plan requirements.

#### 1.2.2.5 Task 13.0 – Maintenance & Refinement of Pressure Core Transport, Storage, & Manipulation Capability

**Status:** Ongoing

- During this quarter, UT scanned and conducted a sampling of core H005-2FB-2. In March, 2020, UT identified several K0 operational deficiencies which involved scratches on sealing surfaces, bottom cap seal failures, high motor torque values, and reduced axial loading capability. Geotek provided a series of procedures to remedy these deficiencies. These remedies were used in the testing of the H005-2FB-2 sample. Scratching and high torque values were not exhibited. However, UT was unable to achieve sealing of the K0 bottom cap and generate hydraulic axial loading.
- UT continues work to resolve the K0 bottom cap sealing issue, with assistance from Geotek.
- To get a load cell with a higher measurement range, UT has purchased two, higher scale load cells from Geotek to remedy the maxed out load cell readings identified during the K0 dummy sample testing last quarter. On August 17, 2020, another meeting was conducted with Geotek to update them on the status of the remedies testing.
- In Q3, 2020, the K0 remedies were applied to the K0 testing of H005-2FB-2-1 (real pressure core test). The sample was extruded with low motor torque. We were able to seal the sample sleeve and unable to seal the bottom cap. The failure to seal the bottom cap prevented axial loading of the sample via hydraulic pressure behind the bottom cap. In addition, the bottom cap was carrying standard O-ring seals. The test is still ongoing.
- Further testing will work to identify the proper type of seals necessary to allow sealing of the bottom cap. Once bottom cap sealing has been achieved, axial loading of a pressure core sample will be tested using hydraulic pressure.

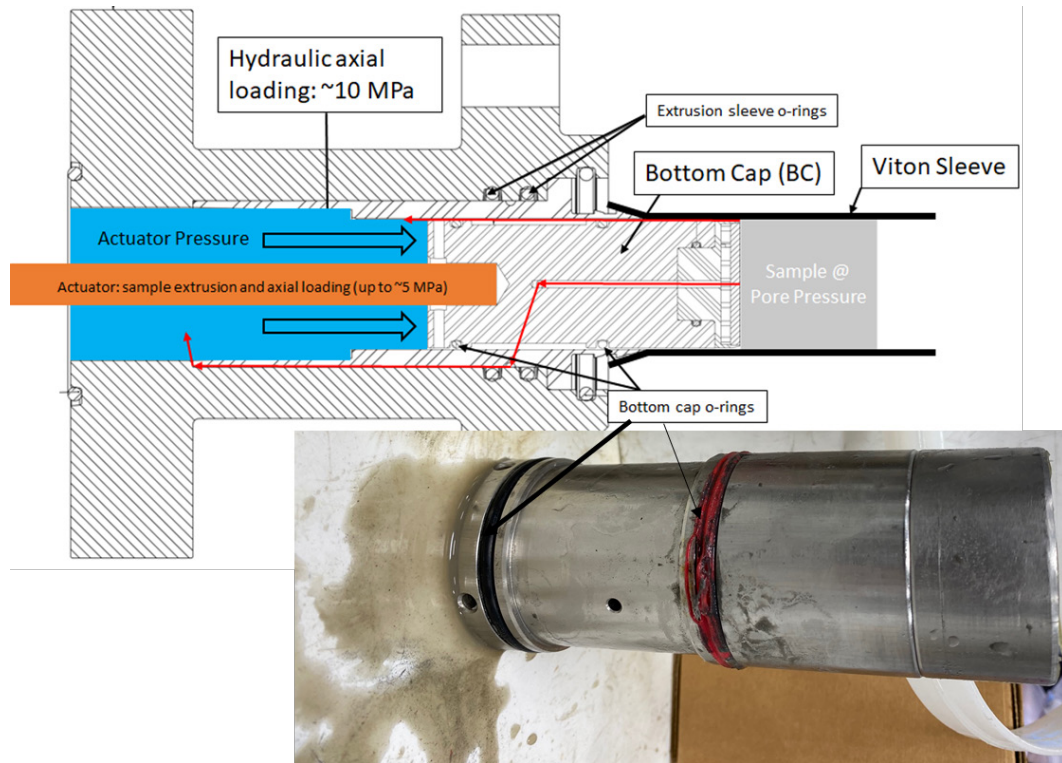


Figure 1-7. Schematic and image of the portion of the KO that needs to seal more consistently. We are able to seal the bottom cap using clean, dummy core samples. We are unable to consistently seal the bottom cap when we move to gritty pressure cores from UT-GOM2-1. Fluid communication was seen between pore fluid and actuator fluid. It is possible that fluid is flowing as indicated by the red arrows in the schematic. A variety of different seal types have been tested during pressure core tests and sealing still fails.

#### 1.2.2.5.1 Subtask 13.1 – Hydrate Core Manipulator and Cutter Tool

- One core was scanned and subsampled with the aid of the new CT scanner system:
  1. Core H005-2FB-2
    - One KO sample
- System underwent its yearly, full maintenance teardown with replacement of seals and bearings. In addition to the cleaning of mPCATS sediment traps.

#### 1.2.2.5.2 Subtask 13.2 – Hydrate Core Effective Stress Chamber

- One pressure core sample continues to undergo long-term KO testing:
  1. H005-2FB-2 - Sample has undergone permeability testing with the presence of hydrate. Then the hydrate was dissolved out of the sample while maintaining an axial load and radial effective stress. The sample will then undergo permeability testing without the presence of hydrate.
- System underwent cleaning between tests. All seals were replaced.
- System is due for full, maintenance teardown next quarter.

#### *1.2.2.5.3 Subtask 13.3 – Hydrate Core Depressurization Chamber*

- UT degassed one sample during this period:
  1. H005-7FB-3-8 – Final remnant of 7FB-3, underwent rapid degassing in July, 2020.
- The system underwent maintenance and cleaning.
- The system was then used to quantify dissolved and dissociated methane hydrate from H005-2FB-2.

#### *1.2.2.5.4 Subtask 13.4 – Develop Hydrate Core Transport Capability for UT-GOM2-2*

- No update this period.

#### *1.2.2.5.5 Subtask 13.5 – Expansion of Pressure Core Storage Capability for UT-GOM2-2*

- New core chamber orientation supports are undergoing design refinement. UT is reviewing quotes to manufacture.
- Expansion of pressure maintenance system is required to increase storage capability sufficient to receive UT-GOM2-2 cores. UT is reviewing quotes for additional pressure lines.
- Expansion of pressure safety venting system will also be required. UT is reviewing quotes for additional venting lines.

#### *1.2.2.5.6 Subtask 13.6 – Continued Storage of Hydrate Cores from UT-GOM2-1*

- Core storage expansion in the PCC is anticipated to accommodate any remaining pressure cores acquired from UT-GOM2-1, even when additional cores are collected during UT-GOM2-2 and transferred to the PCC.

#### *1.2.2.5.7 Subtask 13.7 – X-ray Computed Tomography*

- The X-Ray CT continues to operate as designed.
- During this period, the system was disconnected from mPCATS and all of the wet components cleaned and the seals replaced.

#### *1.2.2.5.8 Subtask 13.8 – Pre-Consolidation System*

- One of the Pre-Consolidation System hydraulic accumulators has developed a leak at the gas charging port. Replacement parts have been quoted and ordered from Geotek LTD.

### **1.2.2.6 Task 14.0 – Performance Assessment, Modifications, And Testing Of PCTB**

**Status:** Ongoing

#### *1.2.2.6.1 Subtask 14.1 – PCTB Lab Test*

- Task Complete

#### *1.2.2.6.2 Subtask 14.2 – PCTB Modifications/Upgrades*

- Task Complete

#### *1.2.2.6.3 Subtask 14.3 – PCTB Land Test*

- Task Complete

#### *1.2.2.6.4 Subtask 14.4 – Other – Continued PCTB Testing and Modification*

- Geotek continued to evaluate the PCTB ball-valve behavior at the Geotek testing facilities in Salt Lake City, Utah.
- The failure of the PCTB to seal is interpreted to be caused by foreign particles (grit/fine sand) becoming lodged in the seal carrier and ball follower, causing the ball not to seal upon actuation.
- Geotek developed an approach to observed ball valve closure in the presence of sediment. The ball valve mechanism is encapsulated in a transparent polycarbonate test fixture and actuated while being video-recorded at high frames-per-second and evaluated in slow-motion playback.
- Geotek conducted ball-valve actuation tests with water and mud loaded with varying amounts of medium and fine sand. Geotek has achieved grit-induced ball-valve failure on a repeatable basis in the ball-valve actuation tests. The observations made during these tests led to a series of proposed design changes to the ball-valve assembly.

The following issues were identified by Geotek as increasing the susceptibility of ball-valve jamming in the current version of the PCTB (PCTB Mk 4):

1. Jamming from fine grit between sliding surface (seal carrier and ball valve housing, ball follower and ball valve housing, and cutting shoe sleeve and ball follower).
2. Flow paths streamline fine grit particles into sliding surfaces
3. Insufficient flow through housing extension to prevent bit balling of cutting shoe ports
4. No cleaning or protection mechanism to prevent jamming
5. Centralization problems allow for seal carrier misalignment during actuation
6. Over-compressed ball valve return spring contributes to jamming
7. Geotek developed provisional design solutions to this problem, and manufactured parts for tests. Geotek then designed a procedure to test each modification individually.

Geotek designed, fabricated, and incrementally tested the proposed upgrades to the PCTB (PCTB Mk 5):

1. Extended seal carrier shoulder for improved centralization during actuation
2. One low friction lip seal on seal carrier
3. Seal carrier and ball follower wiper ring for diverting grit and cleaning surfaces during actuation

4. Extended ball follower shoulder for maintaining contact with wiper ring during actuation
5. Milled slots in ball follower for fluid compensation to prevent hydro locking
6. Short ball valve return spring with fewer coils to prevent jamming
7. Extended cutting shoe sleeve for repositioning of diversion seal
8. ID sealing diversion Polypack to verify flow is not routed into sliding surfaces
9. Steeper angled flow ports on housing extension for improved flow paths to cutting shoe flow ports

In early September, Geotek completed a proof-of-concept PCTB assembly that included all of the PCTB Mk 5 upgrades. On September 29-30, Geotek conducted a series of demonstration tests with Tom Pettigrew of Pettigrew Engineering in attendance. A group of isolated ball valve testing was performed with two different ball valve assemblies. The first ball valve assembly was the Mk 4 version of the tool, used during the PCTB Land Test II. The second ball valve assembly used was the Mk 5 version which includes the design upgrades intended to eliminate the ball-valve failures observed in the PCTB Land Test II. Each test included a water and grit solution with two different quantities of fine grit (53-125  $\mu\text{m}$  particle size). The first quantity of grit uses 0.05 lbs of fine grit per 2.5 gallons of water. This ratio was identical to the 0.24% solids by weight extracted from the CTF 2020 mud samples. The second quantity of grit used was 0.15 lbs of grit per 2.5 gallons of water, this quantity was used to evaluate how well the design modifications could perform in extreme conditions.

Four ball-valve actuation tests were conducted with the PCTB Mk 4. 0/4 tests with the PCTB Mk4 were successful. Thirteen ball-valve actuation tests were conducted with the PCTB Mk 5. 8/13 PCTB Mk 5 tests were successful. The Mk 5 ball valve initially passed 3/6 tests, after which Geotek recognized that the wiper ring seals being used were out of spec. The seals were replaced and testing continued. The Mk 5 ball valve passed 3/3 additional tests using in-spec seals. The Mk 5 ball valve was then tested in more extreme conditions using 3X the amount of grit observed at CTF. This group passed 2/4 tests. In each failed Mk 5 test, the ball valve completed stroke when a small amount of downward pressure was applied or the assembly was rattled. A summary of the PCTB Mk 5 test results is provided below. More information is provided in **Attachment B**.

#### **PCTB Mk5 Test Results:**

##### **Initial tests with out of spec seals (3/6 pass)**

**Test 1:** Failure, ball valve closes approximately 60%

**Test 2:** Pass, full closure, actuation was smooth with no interruptions

**Test 3:** Pass, full closure, actuation was smooth with no interruptions

**Test 4:** Failure, approximately 90% closure. Ball valve finished actuation after applying downward pressure

**Test 5:** Pass, full closure, actuation was smooth with no interruptions

**Test 6:** Failure, approximately 90% closure. Ball valve finished actuation after applying downward pressure

##### **Continued tests with changed seals (3/3 pass)**

**Test 7:** Pass, full closure, actuation was smooth with no interruptions

**Test 8:** Pass, full closure, actuation was smooth with no interruptions

**Test 9:** Pass, full closure, actuation was smooth with no interruptions

**Grit increased 3X (2/4 pass)**

**Test 10:** Pass, full closure, actuation was smooth with no interruptions

**Test 11:** Pass, full closure, actuation was smooth with no interruptions

**Test 12:** Failure, approximately 90% closure. Ball valve finished actuation after applying downward pressure

**Test 13:** Failure, approximately 90% closure. Ball valve finished actuation after lightly rattling

A final test (test 14) was performed on the PCTB Mk 5 in the downhole test chamber. The purpose of this test was to validate that there were no issues during full downhole actuation with the modified Mk 5 ball valve. The results of this test demonstrated successful ball-valve actuation and sealing in the downhole pressure chamber.

### 1.2.2.7 Task 15.0 – UT-GOM2-2 Scientific Drilling Program Preparations

**Status:** In Progress

#### 1.2.2.7.1 Subtask 15.3 – Permitting for UT-GOM2-2 Scientific Drilling Program

- The UT-GOM2-2 Permit Team (consisting of UT and Ohio State) continued to hold weekly web conferences to work on permits for the H002 and G002 that will be drilled as part of the UT-GOM2-2 Scientific Drilling Program. UT and Ohio State also continued work on the F001 and F002 well permits that will be permitted, but only drilled if additional funding is available.
- The Permitting Team collaborated with the Science and Core Analysis Team on technical issues, including:
  1. The committed plan for coring points
  2. Maximum number of cores per well based on processing and storage limitations
  3. Contingency coring plans to respond to different geological scenarios at possible updip location
  4. Time, mud, and resources estimates for each well
- UT developed the blowout scenario (conditions required to encounter free gas leg(s) due to trajectory deviation
- UT and Ohio State completed the Geology and Geophysical (G&G) chapter of the BOEM Exploration Plan.
- UT and Ohio State completed a Shallow Hazard Assessment report for each proposed UT-GOM2-2 drilling location, pursuant to 30 CFR 250.214(f) and 250.244 (f). The Shallow Hazard Reports will accompany the UT-GOM2-2 BOEM Exploration Plan.
- UT and Pettigrew Engineering developed detailed time, mud, and resource estimates for the ‘base-case’ scenario of each well, allowance cores, and contingency cases.

## 1.3 What Will Be Done In The Next Reporting Period To Accomplish These Goals

### 1.3.1 Task 1.0 – Project Management & Planning

UT will continue to execute the project in accordance with the approved PMP. UT will continue to manage and control project activities in accordance with their established processes and procedures to ensure subtasks and tasks are completed within schedule and budget constraints defined by the PMP.

### 1.3.2 Task 10.0 – Core Analysis

- Work will continue on measuring the petrophysical and geomechanical properties of pressure cores using the UT K0 Permeameter (core 2FB-2-1). We are at the very end stage of this test. We have dissolved all hydrate in the core sample 2FB-2-1. We will run an intrinsic permeability test on the hydrate-free core sample.
- Quantitative degassing will continue as needed in support of the permeability measurements and to acquire additional gas samples for carbon, hydrogen, and noble gas isotopic analysis at Ohio State.
- Work will continue on quantifying core degradation during long-term storage.
- Work will continue on finalizing and posting Data Reports
- UT, Ohio State, and the University of New Hampshire continue working on contributions to the AAPG Special Bulletin Volumes (2, and 3).
- Ohio State will measure the gas geochemistry of bulk gas samples from H005-07FB-3, 49-66 cm and H005-2FB2, 5-32 cm.
- UNH plans to finish remeasurement of sediment TOC once their lab reopens.
- Oregon State with Texas A&M Corpus Christi will continue assessing the microbial communities in GC 955 sediment as possible depending on how long labs are shut down.

### 1.3.3 Task 11.0 – Update Operations Plan for UT-GOM2-2 Scientific Drilling Program

- UT and Ohio State will continue to update the operations plan, as required, based on changes to the Exploration Plan, vessel specification, and Science and Sample Distribution Plan.
- UT will continue to develop the UT-GOM2-2 Science and Sample Distribution Plan incorporating recommendations from the TAG and the Core Analysis Team.

### 1.3.4 Task 12.0 – UT-GOM2-2 Scientific Drilling Program Vessel Access

- UT will complete the vessel specification document.
- UT will continue to finalize and initiate execution of the UT-GOM2-2 vessel procurement plan.

### *1.3.5 Task 13.0 – Maintenance And Refinement Of Pressure Core Transport, Storage, & Manipulation Capability*

- The Mini-PCATS, PMRS, analytical equipment, and all storage chambers will undergo continued observation and maintenance at regularly scheduled intervals and on an as-needed basis.
- After successful proof of concept and dummy sample testing, UT has continued to conduct testing of the Geotek remedies to ensure their viability with real world pressure core analysis.
- In addition to real world testing, UT will pursue a small, clear, acrylic testing chamber in an attempt to observe K0 bottom cap sealing in real world environmental conditions without the expense of using real pressure cores.

### *1.3.6 Task 14.0 – Performance Assessment, Modifications, And Testing Of PCTB*

- UT will continue to coordinate with Geotek in their independent evaluation and post-Land Test testing of the PCTB.
- Geotek will continue to perform additional evaluation of the PCTB Mk 5 ball-valve, including design and testing of further modifications based on the outcome of the PCTB Mk 5 tests performed in September.
- UT will monitor the results of Geotek’s ongoing evaluation, and report updates immediately to the PCTB Development Team.
- UT will engage the PCTB Development Team (including members of DOE and USGS) to determine what additional testing of the PCTB will be required prior to deployment during UT-GOM2-1.

### *1.3.7 Task 15.0 – UT-GOM2-2 Scientific Drilling Program Preparations*

- The UT-GOM2-2 Permitting Team will continue to hold weekly web-conferences to work through permit-related issues.
- We will submit the Exploration Plan (EP), Right-of-Use-and-Easement (RUE), and Geological and Geophysical (G&G) permit documents and Shallow Hazards Assessments to BOEM.

## 2 PRODUCTS

Project publications webpage: <https://ig.utexas.edu/energy/gom2-methane-hydrates-at-the-university-of-texas/gom2-publications/>

### 2.1 Publications

- Boswell, R., Collet, T.C., Cook, A.E., Flemings, P.B., 2020, Introduction to Special Issue: Gas Hydrates in Green Canyon Block 955, deep-water Gulf of Mexico: Part I: AAPG Bulletin, v. 104, no. 9, p. 1844-1846, <http://dx.doi.org/10.1306/bltnintro062320>.
- Chen, X., and Espinoza, D. N., 2018a, Ostwald ripening changes the pore habit and spatial variability of clathrate hydrate: Fuel, v. 214, p. 614-622. <https://doi.org/10.1016/j.fuel.2017.11.065>
- Chen, X., Verma, R., Espinoza, D. N., and Prodanović, M., 2018, Pore-Scale Determination of Gas Relative Permeability in Hydrate-Bearing Sediments Using X-Ray Computed Micro-Tomography and Lattice Boltzmann Method: Water Resources Research, v. 54, no. 1, p. 600-608. <https://doi.org/10.1002/2017wr021851>
- Chen, X. Y., and Espinoza, D. N., 2018b, Surface area controls gas hydrate dissociation kinetics in porous media: Fuel, v. 234, p. 358-363. <https://doi.org/10.1016/j.fuel.2018.07.030>
- Cook, A. E., and Portnov, A., 2019, Gas hydrates in coarse-grained reservoirs interpreted from velocity pull up: Mississippi Fan, Gulf of Mexico: COMMENT: Geology, v. 47, no. 3, p. e457-e457. <https://doi.org/10.1130/g45609c.1>
- Cook, A. E., and Sawyer, D. E., 2015, The mud-sand crossover on marine seismic data: Geophysics, v. 80, no. 6, p. A109-A114. <https://doi.org/10.1190/geo2015-0291.1>
- Cook, A. E., and Waite, W. F., 2018, Archie's Saturation Exponent for Natural Gas Hydrate in Coarse-Grained Reservoirs, v. 123, no. 3, p. 2069-2089. <https://doi.org/10.1002/2017jb015138>
- Darnell, K. N., and Flemings, P. B., 2015, Transient seafloor venting on continental slopes from warming-induced methane hydrate dissociation: Geophysical Research Letters, p. n/a-n/a. <https://doi.org/10.1002/2015GL067012>
- Darnell, K. N., Flemings, P. B., and DiCarlo, D., 2019, Nitrogen-Driven Chromatographic Separation During Gas Injection Into Hydrate-Bearing Sediments: Water Resources Research. <https://doi.org/10.1029/2018wr023414>
- Ewton, E., 2019, The effects of X-ray CT scanning on microbial communities in sediment cores [Honors]: Oregon State University, 21 p.
- Fang, Y., Flemings, P. B., Daigle, H., Phillips, S. C., Meazell, P. K., and You, K., 2020, Petrophysical properties of the Green Canyon block 955 hydrate reservoir inferred from reconstituted sediments: Implications for hydrate formation and production: AAPG Bulletin, v. 104, no. 9, p. 1997-2028, <https://doi.org/10.1306/01062019165>
- Flemings, P. B., Phillips, S. C., Boswell, R., Collett, T. S., Cook, A. E., Dong, T., Frye, M., Guerin, G., Goldberg, D. S., Holland, M. E., Jang, J., Meazell, K., Morrison, J., O'Connell, J., Pettigrew, T., Petrou, E., Polito, P. J., Portnov, A., Santra, M., Schultheiss, P. J., Seol, Y., Shedd, W., Solomon, E. A., Thomas, C., Waite, W. F., and You, K., 2020, Pressure coring a Gulf of Mexico Deepwater Turbidite Gas Hydrate Reservoir: Initial results from the UT-GOM2-1 hydrate pressure coring expedition: AAPG Bulletin, v. 104, no. 9, p. 1847-1876. <https://doi.org/10.1306/05212019052>
- Flemings, P. B., Phillips, S. C., Collett, T., Cook, A., Boswell, R., and Scientists, U.-G.-E., 2018, UT-GOM2-1 Hydrate Pressure Coring Expedition Summary, in Flemings, P. B., Phillips, S. C., Collett, T., Cook, A., Boswell, R., and Scientists, U.-G.-E., eds., UT-GOM2-1 Hydrate Pressure Coring Expedition Report: Austin, TX, University of Texas Institute for Geophysics.

- Hillman, J. I. T., Cook, A. E., Daigle, H., Nole, M., Malinverno, A., Meazell, K., and Flemings, P. B., 2017a, Gas hydrate reservoirs and gas migration mechanisms in the Terrebonne Basin, Gulf of Mexico: *Marine and Petroleum Geology*, v. 86, no. Supplement C, p. 1357-1373. <https://doi.org/10.1016/j.marpetgeo.2017.07.029>
- Hillman, J. I. T., Cook, A. E., Sawyer, D. E., Küçük, H. M., and Goldberg, D. S., 2017b, The character and amplitude of 'discontinuous' bottom-simulating reflections in marine seismic data: *Earth and Planetary Science Letters*, v. 459, p. 157-169. <https://doi.org/10.1016/j.epsl.2016.10.058>
- Majumdar, U., and Cook, A. E., 2018, The Volume of Gas Hydrate-Bound Gas in the Northern Gulf of Mexico: *Geochemistry, Geophysics, Geosystems*, v. 19, no. 11, p. 4313-4328. <https://doi.org/10.1029/2018gc007865>
- Majumdar, U., Cook, A. E., Shedd, W., and Frye, M., 2016, The connection between natural gas hydrate and bottom-simulating reflectors: *Geophysical Research Letters*. <https://doi.org/10.1002/2016GL069443>
- Meazell, K., Flemings, P., Santra, M., and Johnson, J. E., 2020, Sedimentology and stratigraphy of a deepwater gas hydrate reservoir in the northern Gulf of Mexico: *AAPG Bulletin*, v. 104, no. 9, p. 1945–1969, <https://doi.org/10.1306/05212019027>
- Meyer, D. W., 2018, Dynamics of gas flow and hydrate formation within the hydrate stability zone [Doctor of Philosophy: The University of Texas at Austin.
- Meyer, D. W., Flemings, P. B., and DiCarlo, D., 2018a, Effect of Gas Flow Rate on Hydrate Formation Within the Hydrate Stability Zone: *Journal of Geophysical Research-Solid Earth*, v. 123, no. 8, p. 6263-6276. <https://doi.org/10.1029/2018jb015878>
- Meyer, D. W., Flemings, P. B., DiCarlo, D., You, K. H., Phillips, S. C., and Kneafsey, T. J., 2018b, Experimental Investigation of Gas Flow and Hydrate Formation Within the Hydrate Stability Zone: *Journal of Geophysical Research-Solid Earth*, v. 123, no. 7, p. 5350-5371. <https://doi.org/10.1029/2018jb015748>
- Moore, M., Phillips, S., Cook, A.E. and Darrah, T., (2020) Improved sampling technique to collect natural gas from hydrate-bearing pressure cores. *Applied Geochemistry*, Volume 122, November 2020, p. 104773, <https://doi.org/10.1016/j.apgeochem.2020.104773>.
- Phillips, S. C., Flemings, P. B., Holland, M. E., Schulthiss, P. J., Waite, W. F., Jang, J., Petrou, E. G., and H., H., 2020, High concentration methane hydrate in a silt reservoir from the deep-water Gulf of Mexico: *AAPG Bulletin*, v. 104, no. 9, p. 1971–1995. <https://doi.org/10.1306/01062018280>
- Phillips, S. C., Flemings, P. B., You, K., Meyer, D. W., and Dong, T., 2019, Investigation of in situ salinity and methane hydrate dissociation in coarse-grained sediments by slow, stepwise depressurization: *Marine and Petroleum Geology*, v. 109, p. 128-144. <https://doi.org/10.1016/j.marpetgeo.2019.06.015>
- Portnov, A., Cook, A. E., Heidari, M., Sawyer, D. E., Santra, M., and Nikolinakou, M., 2020, Salt-driven evolution of a gas hydrate reservoir in Green Canyon, Gulf of Mexico: *AAPG Bulletin*, v. 104, no. 9, p. 1903–1919, <http://dx.doi.org/10.1306/10151818125>
- Portnov, A., Cook, A. E., Sawyer, D. E., Yang, C., Hillman, J. I. T., and Waite, W. F., 2019, Clustered BSRs: Evidence for gas hydrate-bearing turbidite complexes in folded regions, example from the Perdido Fold Belt, northern Gulf of Mexico: *Earth and Planetary Science Letters*, v. 528. <https://doi.org/10.1016/j.epsl.2019.115843>
- Santra, M., Flemings, P., Meazell, K., and Scott, E., 2020, Evolution of Gas Hydrate-bearing Deepwater Channel-Levee System in Abyssal Gulf of Mexico – Levee Growth and Deformation: : *AAPG Bulletin*, v. 104, no. 9, p. 1921–1944, <https://doi.org/doi.org/10.1306/04251918177>
- Sawyer, D. E., Mason, R. A., Cook, A. E., and Portnov, A., 2019, Submarine Landslides Induce Massive Waves in Subsea Brine Pools: *Scientific Reports*, v. 9, no. 1, p. 128. <https://doi.org/10.1038/s41598-018-36781-7>
- Sheik, C. S., Reese, B. K., Twing, K. I., Sylvan, J. B., Grim, S. L., Schrenk, M. O., Sogin, M. L., and Colwell, F. S., 2018, Identification and Removal of Contaminant Sequences From Ribosomal Gene Databases: Lessons From the Census of Deep Life: *Front Microbiol*, v. 9, p. 840. <https://doi.org/10.3389/fmicb.2018.00840>

- Smart, K (2018). Modeling Well Log Responses in Hydrate Bearing Silts. Ohio State University. Undergraduate Thesis.
- Smith, A. J., Flemings, P. B., Liu, X., and Darnell, K., 2014, The evolution of methane vents that pierce the hydrate stability zone in the world's oceans: *Journal of Geophysical Research: Solid Earth*, p. 2013JB010686. <https://doi.org/10.1002/2013JB010686>
- Thomas, C., Phillips, S. C., Flemings, P. B., Santra, M., Hammon, H., Collett, T. S., Cook, A., Pettigrew, T., Mimitz, M., Holland, M., and Schultheiss, P., 2020, Pressure-coring operations during the University of Texas Hydrate Pressure Coring Expedition, UT-GOM2-1, in Green Canyon Block 955, northern Gulf of Mexico: *AAPG Bulletin*, v. 104, no. 9, p. 1877–1901. <https://doi.org/10.1306/02262019036>
- Wei, L., Cook, A., Daigle, H., Malinverno, A., Nole, M., and You, K., 2019, Factors Controlling Short-Range Methane Migration of Gas Hydrate Accumulations in Thin Coarse-Grained Layers: *Geochemistry, Geophysics, Geosystems*, v. 20, no. 8, p. 3985–4000. <https://doi.org/10.1029/2019gc008405>
- You, K., and Flemings, P. B., 2018, Methane hydrate formation in thick sandstones by free gas flow: *Journal of Geophysical Research: Solid Earth*, v. 123, p. 4582–4600. <https://doi.org/10.1029/2018JB015683>
- You, K., Flemings, P. B., Malinverno, A., Collett, T. S., and Darnell, K., 2019, Mechanisms of Methane Hydrate Formation in Geological Systems: *Reviews of Geophysics*, v. 0, no. ja. <https://doi.org/10.1029/2018rg000638>
- You, K., Kneafsey, T. J., Flemings, P. B., Polito, P., and Bryant, S. L., 2015, Salinity-buffered methane hydrate formation and dissociation in gas-rich systems: *Journal of Geophysical Research: Solid Earth*, v. 120, no. 2, p. 643–661. <https://doi.org/10.1002/2014JB011190>

## 2.2 Conference Presentations/Abstracts

- Cook, A., Waite, W. F., Spangenberg, E., and Heeschen, K.U., 2018, Petrophysics in the lab and the field: how can we understand gas hydrate pore morphology and saturation? Invited talk presented at the American Geophysical Union Fall Meeting, Washington D.C.
- Cook, A.E., and Waite, B., 2016, Archie's saturation exponent for natural gas hydrate in coarse-grained reservoir. Presented at Gordon Research Conference, Galveston, TX.
- Cook, A.E., Hillman, J., Sawyer, D., Treiber, K., Yang, C., Frye, M., Shedd, W., Palmes, S., 2016, Prospecting for Natural Gas Hydrate in the Orca & Choctaw Basins in the Northern Gulf of Mexico. Poster presented at American Geophysical Union, Fall Meeting, San Francisco, CA.
- Cook, A.E., Hillman, J., & Sawyer, D., 2015, Gas migration in the Terrebonne Basin gas hydrate system. Abstract OS23D-05 presented at American Geophysical Union, Fall Meeting, San Francisco, CA.
- Cook, A. E., & Sawyer, D., 2015, Methane migration in the Terrebonne Basin gas hydrate system, Gulf of Mexico. Presented at American Geophysical Union, Fall Meeting, San Francisco, CA.
- Chen X., Espinoza, D.N., Tisato, N., and Flemings, P.B., 2018, X-Ray Micro-CT Observation of Methane Hydrate Growth in Sandy Sediments. Presented at the AGU Fall Meeting 2018, Dec. 10–14, in Washington D.C.
- Darnell, K., Flemings, P.B., DiCarlo, D.A., 2016, Nitrogen-assisted Three-phase Equilibrium in Hydrate Systems Composed of Water, Methane, Carbon Dioxide, and Nitrogen. Presented at American Geophysical Union, Fall Meeting, San Francisco, CA.
- Dong, T., Lin, J. -F., Flemings, P. B., Gu, J. T., Polito, P. J., O'Connell, J., 2018, Pore-Scale Methane Hydrate Formation under Pressure and Temperature Conditions of Natural Reservoirs. Presented to the AGU Fall Meeting 2018, Washington D.C., 10-14 December.

- Ewton, E., Klasek, S., Peck, E., Wiest, J. Colwell F., 2019, The effects of X-ray computed tomography scanning on microbial communities in sediment cores. Poster presented at AGU Fall Meeting.
- Erica Ewton et al., 2018, The effects of X-ray CT scanning on microbial communities in sediment cores. Poster presented at American Geophysical Union, Fall Meeting, Washington, D.C. OS23D-1657
- Espinoza D.N., Chen X., Luo J.S., Tisato N., Flemings P.B., 2010, X-Ray Micro-CT Observation of Methane Hydrate Growth and Dissociation in Sandy Sediments. Presented to the Engineering Mechanics Institute Conference 2019, Pasadena, CA, 19 June.
- Fang, Y., et al., 2020, Petrophysical Properties of Hydrate-Bearing Siltstone from UT-GOM2-1 Pressure Cores. Presented at the AAPG virtual Conference, Oct 1, Theme 9: Analysis of Natural Gas Hydrate Systems I & II
- Fang, Y., et al., 2018, Permeability, compression behavior, and lateral stress ration of hydrate-bearing siltstone from UT-GOM2-1 pressure core (GC-955 – northern Gulf of Mexico): Initial Results. Poster presented at American Geophysical Union, Fall Meeting, Washington, D.C. OS23D-1650
- Fang, Y., Flemings, P.B., Daigle, H., O'Connell, J., Polito, P., 2018, Measure permeability of natural hydrate-bearing sediments using K0 permeameter. Presented at Gordon Research Conference on Gas Hydrate, Galveston, TX. Feb 24- Mar 02, 2018.
- Flemings, P.B., et al., 2020 Pressure Coring a Gulf of Mexico Deep-Water Turbidite Gas Hydrate Reservoir: The UT-GOM2-1 Hydrate Pressure Coring Expedition. Presented at the AAPG virtual Conference, Oct 1, Theme 9: Analysis of Natural Gas Hydrate Systems I & II
- Flemings, P., Phillips, S., and the UT-GOM2-1 Expedition Scientists, 2018, Recent results of pressure coring hydrate-bearing sands in the deepwater Gulf of Mexico: Implications for formation and production. Talk presented at the 2018 Gordon Research Conference on Natural Gas Hydrate Systems, Galveston, TX, February 24-March 2, 2018.
- Fortin, W., 2018, Waveform Inversion and Well Log Examination at GC955 and WR313 in the Gulf of Mexico for Estimation of Methane Hydrate Concentrations. Presented at Gordon Research Conference on Natural Gas Hydrate Systems, Galveston, TX.
- Fortin, W., Goldberg, D.S., Küçük, H. M., 2017, Prestack Waveform Inversion and Well Log Examination at GC955 and WR313 in the Gulf of Mexico for Estimation of Methane Hydrate Concentrations. EOS Trans. American Geophysical Union, Fall Meeting, New Orleans, LA.
- Fortin, W., 2016, Properties from Seismic Data. Presented at IODP planning workshop, Southern Methodist University, Dallas, TX.
- Fortin, W., Goldberg, D.S., Holbrook, W.S., and Küçük, H.M., 2016, Velocity analysis of gas hydrate systems using prestack waveform inversion. Presented at Gordon Research Conference on Natural Gas Hydrate Systems, Galveston, TX.
- Fortin, W., Goldberg, D.S., Küçük, H.M., 2016, Methane Hydrate Concentrations at GC955 and WR313 Drilling Sites in the Gulf of Mexico Determined from Seismic Prestack Waveform Inversion. EOS Trans. American Geophysical Union, Fall Meeting, San Francisco, CA.
- Goldberg, D., Küçük, H.M., Haines, S., Guerin, G., 2016, Reprocessing of high resolution multichannel seismic data in the Gulf of Mexico: implications for BSR character in the Walker Ridge and Green Canyon areas. Presented at Gordon Research Conference on Natural Gas Hydrate Systems, Galveston, TX.
- Hammon, H., Phillips, S., Flemings, P., and the UT-GOM2-1 Expedition Scientists, 2018, Drilling-induced disturbance within methane hydrate pressure cores in the northern Gulf of Mexico. Poster presented at

- the 2018 Gordon Research Conference and Seminar on Natural Gas Hydrate Systems, Galveston, TX, February 24-March 2, 2018.
- Heber, R., Kinash, N., Cook, A., Sawyer, D., Sheets, J., and Johnson, J.E., 2017, Mineralogy of Gas Hydrate Bearing Sediment in Green Canyon Block 955 Northern Gulf of Mexico. Abstract OS53B-1206 presented at American Geophysical Union, Fall Meeting, New Orleans, LA.
- Hillman, J., Cook, A. & Sawyer, D., 2016, Mapping and characterizing bottom-simulating reflectors in 2D and 3D seismic data to investigate connections to lithology and frequency dependence. Presented at Gordon Research Conference, Galveston, TX.
- Johnson, J., et al., 2020, Grain Size, TOC, and TS in Gas Hydrate Bearing Turbidite Facies at Green Canyon Site 955, Gulf of Mexico. Presented at the AAPG virtual Conference, Oct 1, Theme 9: Analysis of Natural Gas Hydrate Systems I & II
- Johnson, J., 2018, High Porosity and Permeability Gas Hydrate Reservoirs: A Sedimentary Perspective. Presented at Gordon Research Conference on Natural Gas Hydrate Systems, Galveston, TX.
- Kinash, N. Cook, A., Sawyer, D. and Heber, R., 2017, Recovery and Lithologic Analysis of Sediment from Hole UT-GOM2-1-H002, Green Canyon 955, Northern Gulf of Mexico. Abstract OS53B-1207 presented at American Geophysical Union, Fall Meeting, New Orleans, LA.
- Küçük, H.M., Goldberg, D.S, Haines, S., Dondurur, D., Guerin, G., and Çifçi, G., 2016, Acoustic investigation of shallow gas and gas hydrates: comparison between the Black Sea and Gulf of Mexico. Presented at Gordon Research Conference on Natural Gas Hydrate Systems, Galveston, TX.
- Liu, J. et al., 2018, Pore-scale CH<sub>4</sub>-C<sub>2</sub>H<sub>6</sub> hydrate formation and dissociation under relevant pressure-temperature conditions of natural reservoirs. Poster presented at American Geophysical Union, Fall Meeting, Washington, D.C. OS23D-2824
- Malinverno, A., Cook, A. E., Daigle, H., Oryan, B., 2017, Methane Hydrate Formation from Enhanced Organic Carbon Burial During Glacial Lowstands: Examples from the Gulf of Mexico. EOS Trans. American Geophysical Union, Fall Meeting, New Orleans, LA.
- Malinverno, A., 2016, Modeling gas hydrate formation from microbial methane in the Terrebonne basin, Walker Ridge, Gulf of Mexico. Presented at Gordon Research Conference on Natural Gas Hydrate Systems, Galveston, TX.
- Meazell, K., Flemings, P. B., Santra, M., and the UT-GOM2-01 Scientists, 2018, Sedimentology of the clastic hydrate reservoir at GC 955, Gulf of Mexico. Presented at Gordon Research Conference on Natural Gas Hydrate Systems, Galveston, TX.
- Meazell, K., & Flemings, P.B., 2016, Heat Flux and Fluid Flow in the Terrebonne Basin, Northern Gulf of Mexico. Presented at American Geophysical Union, Fall Meeting, San Francisco, CA.
- Meazell, K., & Flemings, P.B., 2016, New insights into hydrate-bearing clastic sediments in the Terrebonne basin, northern Gulf of Mexico. Presented at Gordon Research Conference on Natural Gas Hydrate Systems, Galveston, TX.
- Meazell, K., & Flemings, P.B., 2016, The depositional evolution of the Terrebonne basin, northern Gulf of Mexico. Presented at 5th Annual Jackson School Research Symposium, University of Texas at Austin, Austin, TX.
- Meazell, K., 2015, Methane hydrate-bearing sediments in the Terrebonne basin, northern Gulf of Mexico. Abstract OS23B-2012 presented at American Geophysical Union, Fall Meeting, San Francisco, CA.

- Moore, M., Darrah, T., Cook, A., Sawyer, D., Phillips, S., Whyte, C., Lary, B., and UT-GOM2-01 Scientists, 2017, The genetic source and timing of hydrocarbon formation in gas hydrate reservoirs in Green Canyon, Block GC955. Abstract OS44A-03 presented at American Geophysical Union, Fall Meeting, New Orleans, LA.
- Morrison, J., Flemings, P., and the UT-GOM2-1 Expedition Scientists, 2018, Hydrate Coring in Deepwater Gulf of Mexico, USA. Poster presented at the 2018 Gordon Research Conference on Natural Gas Hydrate Systems, Galveston, TX.
- Murphy, Z., et al., 2018, Three phase relative permeability of hydrate bearing sediments. Poster presented at American Geophysical Union, Fall Meeting, Washington, D.C. OS23D-1647
- Oryan, B., Malinverno, A., Goldberg, D., Fortin, W., 2017, Do Pleistocene glacial-interglacial cycles control methane hydrate formation? An example from Green Canyon, Gulf of Mexico. EOS Trans. American Geophysical Union, Fall Meeting, New Orleans, LA.
- Oti, E., Cook, A., Phillips, S., and Holland, M., 2019, Using X-ray Computed Tomography (XCT) to Estimate Hydrate Saturation in Sediment Cores from UT-GOM2-1 H005, Green Canyon 955 (Invited talk, U11C-17). Presented to the AGU Fall Meeting, San Francisco, CA.
- Oti, E., Cook, A., Phillips, S., Holland, M., Flemings, P., 2018, Using X-ray computed tomography to estimate hydrate saturation in sediment cores from Green Canyon 955 Gulf of Mexico. Talk presented at the American Geophysical Union Fall Meeting, Washington D.C.
- Oti, E., Cook, A., 2018, Non-Destructive X-ray Computed Tomography (XCT) of Previous Gas Hydrate Bearing Fractures in Marine Sediment. Presented at Gordon Research Conference on Natural Gas Hydrate Systems, Galveston, TX.
- Oti, E., Cook, A., Buchwalter, E., and Crandall, D., 2017, Non-Destructive X-ray Computed Tomography (XCT) of Gas Hydrate Bearing Fractures in Marine Sediment. Abstract OS44A-05 presented at American Geophysical Union, Fall Meeting, New Orleans, LA.
- Phillips, S.C., et al., 2020, High Concentration Methane Hydrate in a Silt Reservoir from the Deep-Water Gulf of Mexico. Presented at the AAPG virtual Conference, Oct 1, Theme 9: Analysis of Natural Gas Hydrate Systems I & II
- Phillips, S.C., Formolo, M.J., Wang, D.T., Becker, S.P., and Eiler, J.M., 2020. Methane isotopologues in a high-concentration gas hydrate reservoir in the northern Gulf of Mexico. Goldschmidt Abstracts 2020. <https://goldschmidtabstracts.info/2020/2080.pdf>
- Phillips, S.C., 2019, Pressure coring in marine sediments: Insights into gas hydrate systems and future directions. Presented to the GSA Annual Meeting 2019, Phoenix, Arizona, 22-25 September. <https://gsa.confex.com/gsa/2019AM/meetingapp.cgi/Paper/338173>
- Phillips et al., 2018, High saturation of methane hydrate in a coarse-grained reservoir in the northern Gulf of Mexico from quantitative depressurization of pressure cores. Poster presented at American Geophysical Union, Fall Meeting, Washington, D.C. OS23D-1654
- Phillips, S.C., Flemings, P.B., Holland, M.E., Schultheiss, P.J., Waite, W.F., Petrou, E.G., Jang, J., Polito, P.J., O'Connell, J., Dong, T., Meazell, K., and Expedition UT-GOM2-1 Scientists, 2017, Quantitative degassing of gas hydrate-bearing pressure cores from Green Canyon 955. Gulf of Mexico. Talk and poster presented at the 2018 Gordon Research Conference and Seminar on Natural Gas Hydrate Systems, Galveston, TX, February 24-March 2, 2018.

- Phillips, S.C., Borgfeldt, T., You, K., Meyer, D., and Flemings, P., 2016, Dissociation of laboratory-synthesized methane hydrate by depressurization. Poster presented at Gordon Research Conference and Gordon Research Seminar on Natural Gas Hydrates, Galveston, TX.
- Phillips, S.C., You, K., Borgfeldt, T., Meyer, D.W., Dong, T., Flemings, P.B., 2016, Dissociation of Laboratory-Synthesized Methane Hydrate in Coarse-Grained Sediments by Slow Depressurization. Presented at American Geophysical Union, Fall Meeting, San Francisco, CA.
- Portnov A., et al., 2018, Underexplored gas hydrate reservoirs associated with salt diapirism and turbidite deposition in the Northern Gulf of Mexico. Poster presented at American Geophysical Union, Fall Meeting, Washington, D.C. OS51F-1326
- Portnov, A., Cook, A., Heidari, M., Sawyer, D., Santra, M., Nikolinakou, M., 2018, Salt-driven Evolution of Gas Hydrate Reservoirs in the Deep-sea Gulf of Mexico. Presented at Gordon Research Conference on Natural Gas Hydrate Systems, Galveston, TX.
- Santra, M., et al., 2020, Gas Hydrate in a Fault-Compartmentalized Anticline and the Role of Seal, Green Canyon, Abyssal Northern Gulf of Mexico. Presented at the AAPG virtual Conference, Oct 1, Theme 9: Analysis of Natural Gas Hydrate Systems I & II
- Santra, M., et al., 2018, Channel-levee hosted hydrate accumulation controlled by a faulted anticline: Green Canyon, Gulf of Mexico. Poster presented at American Geophysical Union, Fall Meeting, Washington, D.C. OS51F-1324
- Santra, M., Flemings, P., Scott, E., Meazell, K., 2018, Evolution of Gas Hydrate Bearing Deepwater Channel-Levee System in Green Canyon Area in Northern Gulf of Mexico. Presented at Gordon Research Conference and Gordon Research Seminar on Natural Gas Hydrates, Galveston, TX.
- Treiber, K, Sawyer, D., & Cook, A., 2016, Geophysical interpretation of gas hydrates in Green Canyon Block 955, northern Gulf of Mexico, USA. Poster presented at Gordon Research Conference, Galveston, TX.
- Wei, L. and Cook, A., 2019, Methane Migration Mechanisms and Hydrate Formation at GC955, Northern Gulf of Mexico. Abstract OS41B-1668 presented to the AGU Fall Meeting, San Francisco, CA.
- Worman, S. and, Flemings, P.B., 2016, Genesis of Methane Hydrate in Coarse-Grained Systems: Northern Gulf of Mexico Slope (GOM<sup>2</sup>). Poster presented at The University of Texas at Austin, GeoFluids Consortia Meeting, Austin, TX.
- Yang, C., Cook, A., & Sawyer, D., 2016, Geophysical interpretation of the gas hydrate reservoir system at the Perdido Site, northern Gulf of Mexico. Presented at Gordon Research Conference, Galveston, TX, United States.
- You, K., et al. 2020, Impact of Coupled Free Gas Flow and Microbial Methanogenesis on the Formation and Evolution of Concentrated Hydrate Deposits. Presented at the AAPG virtual Conference, Oct 1, Theme 9: Analysis of Natural Gas Hydrate Systems I & II
- You, K., Flemings, P. B., and Santra, M., 2018, Formation of lithology-dependent hydrate distribution by capillary-controlled gas flow sourced from faults. Poster presented at American Geophysical Union, Fall Meeting, Washington, D.C. OS31F-1864
- You, K., and Flemings, P. B., 2018, Methane Hydrate Formation in Thick Marine Sands by Free Gas Flow. Presented at Gordon Research Conference on Gas Hydrate, Galveston, TX. Feb 24- Mar 02, 2018.
- You, K., Flemings, P.B., 2016, Methane Hydrate Formation in Thick Sand Reservoirs: Long-range Gas Transport or Short-range Methane Diffusion? Presented at American Geophysical Union, Fall Meeting, San Francisco, CA.

You, K.Y., DiCarlo, D. & Flemings, P.B., 2015, Quantifying methane hydrate formation in gas-rich environments using the method of characteristics. Abstract OS23B-2005 presented at 2015, Fall Meeting, AGU, San Francisco, CA, 14-18 Dec.

You, K.Y., Flemings, P.B., & DiCarlo, D., 2015, Quantifying methane hydrate formation in gas-rich environments using the method of characteristics. Poster presented at 2016 Gordon Research Conference and Gordon Research Seminar on Natural Gas Hydrates, Galveston, TX.

## 2.3 Proceeding of the UT-GOM2-1 Hydrate Pressure Coring Expedition

Volume contents are published on the [UT-GOM2-1 Expedition website](#) and on [OSTI.gov](#).

### 2.3.1 Volume Reference

Flemings, P.B., Phillips, S.C, Collett, T., Cook, A., Boswell, R., and the UT-GOM2-1 Expedition Scientists, Proceedings of the UT-GOM2-1 Hydrate Pressure Coring Expedition, Austin, TX (University of Texas Institute for Geophysics, TX), <https://dx.doi.org/10.2172/1646019>

### 2.3.2 Prospectus

Flemings, P.B., Boswell, R., Collett, T.S., Cook, A. E., Divins, D., Frye, M., Guerin, G., Goldberg, D.S., Malinverno, A., Meazell, K., Morrison, J., Pettigrew, T., Philips, S.C., Santra, M., Sawyer, D., Shedd, W., Thomas, C., You, K. GOM2: Prospecting, Drilling and Sampling Coarse-Grained Hydrate Reservoirs in the Deepwater Gulf of Mexico. Proceeding of ICGH-9. Denver, Colorado: ICGH, 2017. <http://www-udc.ig.utexas.edu/gom2/UT-GOM2-1%20Prospectus.pdf>.

### 2.3.3 Expedition Report Chapters

Flemings, P.B., Phillips, S.C, Collett, T., Cook, A., Boswell, R., and the UT-GOM2-1 Expedition Scientists, 2018. UT-GOM2-1 Hydrate Pressure Coring Expedition Summary. In Flemings, P.B., Phillips, S.C, Collett, T., Cook, A., Boswell, R., and the UT-GOM2-1 Expedition Scientists, Proceedings of the UT-GOM2-1 Hydrate Pressure Coring Expedition, Austin, TX (University of Texas Institute for Geophysics, TX). <https://dx.doi.org/10.2172/1647223>.

Flemings, P.B., Phillips, S.C, Collett, T., Cook, A., Boswell, R., and the UT-GOM2-1 Expedition Scientists, 2018. UT-GOM2-1 Hydrate Pressure Coring Expedition Methods. In Flemings, P.B., Phillips, S.C, Collett, T., Cook, A., Boswell, R., and the UT-GOM2-1 Expedition Scientists, Proceedings of the UT-GOM2-1 Hydrate Pressure Coring Expedition: Austin, TX (University of Texas Institute for Geophysics, TX). <https://dx.doi.org/10.2172/1647226>

Flemings, P.B., Phillips, S.C, Collett, T., Cook, A., Boswell, R., and the UT-GOM2-1 Expedition Scientists, 2018. UT-GOM2-1 Hydrate Pressure Coring Expedition Hole GC 955 H002. In Flemings, P.B., Phillips, S.C, Collett, T., Cook, A., Boswell, R., and the UT-GOM2-1 Expedition Scientists, Proceedings of the UT-GOM2-1 Hydrate Pressure Coring Expedition: Austin, TX (University of Texas Institute for Geophysics, TX). <https://dx.doi.org/10.2172/1648313>

Flemings, P.B., Phillips, S.C, Collett, T., Cook, A., Boswell, R., and the UT-GOM2-1 Expedition Scientists, 2018. UT-GOM2-1 Hydrate Pressure Coring Expedition Hole GC 955 H005. In Flemings, P.B., Phillips, S.C, Collett, T., Cook, A., Boswell, R., and the UT-GOM2-1 Expedition Scientists, Proceedings of the UT-GOM2-1 Hydrate Pressure Coring Expedition: Austin, TX (University of Texas Institute for Geophysics, TX).  
<https://dx.doi.org/10.2172/1648318>

### 2.3.4 Data Reports

Fortin, W.F.J., Goldberg, D.S., Küçük, H.M., 2020, Data Report: Prestack Waveform Inversion at GC 955: Trials and sensitivity of PWI to high-resolution seismic data, In Flemings, P.B., Phillips, S.C, Collett, T., Cook, A., Boswell, R., and the UT-GOM2-1 Expedition Scientists, Proceedings of the UT-GOM2-1 Hydrate Pressure Coring Expedition: Austin, TX (University of Texas Institute for Geophysics, TX).  
<http://dx.doi.org/10.2172/1647733>, 7 p.

Heber, R., Cook, A., Sheets, J., Sawyer, 2020. Data Report: High-Resolution Microscopy Images of Sediments from Green Canyon Block 955, Gulf of Mexico. In Flemings, P.B., Phillips, S.C, Collett, T., Cook, A., Boswell, R., and the UT-GOM2-1 Expedition Scientists, Proceedings of the UT-GOM2-1 Hydrate Pressure Coring Expedition: Austin, TX (University of Texas Institute for Geophysics, TX).  
<https://dx.doi.org/10.2172/1648312>, 6 p.

Heber, R., Cook, A., Sheets, J., and Sawyer, D., 2020. Data Report: X-Ray Diffraction of Sediments from Green Canyon Block 955, Gulf of Mexico. In Flemings, P.B., Phillips, S.C, Collett, T., Cook, A., Boswell, R., and the UT-GOM2-1 Expedition Scientists, Proceedings of the UT-GOM2-1 Hydrate Pressure Coring Expedition: Austin, TX (University of Texas Institute for Geophysics, TX). <https://dx.doi.org/10.2172/1648308>, 27 p.

Phillips, I.M., 2018. Data Report: X-Ray Powder Diffraction. In Flemings, P.B., Phillips, S.C, Collett, T., Cook, A., Boswell, R., and the UT-GOM2-1 Expedition Scientists, Proceedings of the UT-GOM2-1 Hydrate Pressure Coring Expedition: Austin, TX (University of Texas Institute for Geophysics, TX).  
<https://dx.doi.org/10.2172/1648320> 14 p.

## 2.4 Websites

- Project Website:

<https://ig.utexas.edu/energy/genesis-of-methane-hydrate-in-coarse-grained-systems/>

- UT-GOM2-1 Expedition Website:

<https://ig.utexas.edu/energy/genesis-of-methane-hydrate-in-coarse-grained-systems/expedition-ut-gom2-1/>

- Project SharePoint:

<https://sps.austin.utexas.edu/sites/GEOMech/doehd/teams/>

- Methane Hydrate: Fire, Ice, and Huge Quantities of Potential Energy:

<https://www.youtube.com/watch?v=f1G302BBX9w>

- Fueling the Future: The Search for Methane Hydrate:

<https://www.youtube.com/watch?v=z1dFc-fdah4>

- Pressure Coring Tool Development Video:

<https://www.youtube.com/watch?v=DXseEbKp5Ak&t=154s>

## 2.5 Technologies Or Techniques

Nothing to report.

## 2.6 Inventions, Patent Applications, and/or Licenses

Nothing to report.

### 3 CHANGES/PROBLEMS

#### 3.1 Changes In Approach And Reasons For Change

Nothing to report.

#### 3.2 Actual Or Anticipated Problems Or Delays And Actions Or Plans To Resolve Them

Nothing to report

#### 3.3 Changes That Have A Significant Impact On Expenditures

Nothing to report.

#### 3.4 Change Of Primary Performance Site Location From That Originally Proposed

Nothing to report.

## 4 SPECIAL REPORTING REQUIREMENTS

### 4.1 Current Project Period

Task 1.0 – Revised Project Management Plan

Task 11.0 – Refined UT-GOM2-2 Scientific Drilling Program Operations Plan

Subtask 14.3 – PCTB Land Test Report

### 4.2 Future Project Periods

Task 1.0 – Revised Project Management Plan

Subtask 15.5 – Final UT-GOM2-2 Scientific Drilling Program Operation Plan

Subtask 17.1 – Project Sample and Data Distribution Plan

Subtask 17.3 – UT-GOM2-2 Scientific Drilling Program Scientific Results Volume

## 5 BUDGETARY INFORMATION

The Budget Period 4 cost summary is provided in Table 5-1.

Table 5-1: Phase 4 / Budget Period 4 Cost Profile

Baseline Reporting Quarter	Budget Period 4							
	Y1Q1		Y1Q2		Y1Q3		Y1Q4	
	10/01/19-12/31/19		01/01/20-03/31/20		04/01/20-06/30/20		07/01/20-09/30/20	
	Y1Q1	Cumulative Total	Y1Q2	Cumulative Total	Y1Q3	Cumulative Total	Y1Q4	Cumulative Total
<b>Baseline Cost Plan</b>								
Federal Share	\$ 1,087,357	\$ 27,293,955	\$ 961,357	\$ 28,255,312	\$ 2,169,274	\$ 30,424,587	\$ 961,357	\$ 31,385,944
Non-Federal Share	\$ 307,598	\$ 22,798,170	\$ 307,598	\$ 23,105,767	\$ 307,598	\$ 23,413,365	\$ 307,598	\$ 23,720,962
<b>Total Planned</b>	<b>\$ 1,394,955</b>	<b>\$ 50,092,125</b>	<b>\$ 1,268,955</b>	<b>\$ 51,361,079</b>	<b>\$ 2,476,872</b>	<b>\$ 53,837,951</b>	<b>\$ 1,268,955</b>	<b>\$ 55,106,906</b>
<b>Actual Incurred Cost</b>								
Federal Share	\$ 266,282	\$ 26,336,093	\$ 1,031,076	\$ 27,367,169	\$ 1,220,967	\$ 28,588,135	\$ 588,610	\$ 29,176,746
Non-Federal Share	\$ 61,210	\$ 22,577,153	\$ 306,656	\$ 22,883,809	\$ 319,211	\$ 23,203,019	\$ 123,925	\$ 23,326,944
<b>Total Incurred Cost</b>	<b>\$ 327,492</b>	<b>\$ 48,913,245</b>	<b>\$ 1,337,732</b>	<b>\$ 50,250,977</b>	<b>\$ 1,540,178</b>	<b>\$ 51,791,155</b>	<b>\$ 712,535</b>	<b>\$ 52,503,690</b>
<b>Variance</b>								
Federal Share	\$ (821,075)	\$ (821,075)	\$ 69,718	\$ (751,357)	\$ (948,307)	\$ (1,699,664)	\$ (372,747)	\$ (2,072,411)
Non-Federal Share	\$ (246,388)	\$ (246,388)	\$ (942)	\$ (247,329)	\$ 11,613	\$ (235,716)	\$ (183,673)	\$ (419,388)
<b>Total Variance</b>	<b>\$ (1,067,463)</b>	<b>\$ (1,067,463)</b>	<b>\$ 68,777</b>	<b>\$ (998,686)</b>	<b>\$ (936,694)</b>	<b>\$ (1,935,380)</b>	<b>\$ (556,420)</b>	<b>\$ (2,491,800)</b>

## 6 ACRONYMS

Table 6-1: List of Acronyms

ACRONYM	DEFINITION
AAPG	American Association of Petroleum Geologists
ACE	Annual Convention and Exhibition
APL	Ancillary Project Letter
BOEM	Bureau of Ocean Energy Management
CFR	Code of Federal Regulation
CPP	Complimentary Project Proposal
CT	Computed Tomography
CTTF	Cameron Test Testing Facility
DOE	U.S. Department of Energy
EP	Exploration Plan
G&G	Geologic and Geophysical
GC	Green Canyon
IODP	International Ocean Discovery Program
JIP	Joint Industry Project
LWD	Logging While Drilling
NEPA	National Environmental Policy Act
NETL	National Energy Technology Laboratory
PCATS	Pressure Core Analysis and Transfer System
PCC	Pressure Core Center
PCTB	Pressure Core Tool with Ball Valve
PCTB-CS	Pressure Core Tool with Ball Valve - Cutting Shoe
PCTB-FB	Pressure Core Tool with Ball Valve - Face Bit
PDT	Probe Deployment Tool
PM	Project Manager
PMP	Project Management Plan
PMRS	Pressure Maintenance and Relief System
QRPPR	Quarterly Research Performance and Progress Report
RPPR	Research Performance and Progress Report
RUE	Right-of-Use-and-Easement
SOPO	Statement of Project Objectives
T2P	Temperature to Pressure Probe
TAG	Technical Advisory Group
TOC	Total Organic Carbon
TS	Total Sulfur
UNH	University of New Hampshire
UT	University of Texas at Austin
UW	University of Washington
XCT	X-ray Computed Tomography
XRD	X-ray Diffraction

## National Energy Technology Laboratory

626 Cochrans Mill Road  
P.O. Box 10940  
Pittsburgh, PA 15236-0940

3610 Collins Ferry Road  
P.O. Box 880  
Morgantown, WV 26507-0880

13131 Dairy Ashford Road, Suite 225  
Sugar Land, TX 77478

1450 Queen Avenue SW  
Albany, OR 97321-2198

Arctic Energy Office  
420 L Street, Suite 305  
Anchorage, AK 99501

Visit the NETL website at:  
[www.netl.doe.gov](http://www.netl.doe.gov)

Customer Service Line:  
1-800-553-7681



U.S. DEPARTMENT OF  
**ENERGY**

**NATIONAL ENERGY  
TECHNOLOGY LABORATORY**

# ATTACHMENT A

Technical Note: UT-GOM2-2 Drilling Fluid

# Technical Note: UT-GOM2-2 Drilling Fluid

Carla Thomas, The University of Texas, Jackson School of Geosciences, Institute for Geophysics, Austin, TX 78712, USA, carla.thomas@utexas.edu

Peter Flemings, The University of Texas, Jackson School of Geosciences, Institute for Geophysics and Department of Geological Sciences, Austin, TX 78712, USA, pflemings@jsg.utexas.edu

Kehua You, The University of Texas, Jackson School of Geosciences, Institute for Geophysics, Austin, TX 78712, USA, kehua@ig.utexas.edu

## 1.0 Executive Summary

It is proposed that a salt-saturated, water-based mud might improve borehole stability for UT-GOM2-2 relative to a fresh-water-based mud. However, the primary objective for UT-GOM2-2 is to safely and successfully acquire uncompromised hydrate-bearing sediment cores. This can only be done if conditions stay within the hydrate stability zone, and well away from the hydrate stability boundary. The addition of salt to the drilling mud, shifts the hydrate stability boundary closer to estimated conditions. This shift, by some estimates of pressure and temperature, where conditions now fall outside of the hydrate stability zone, may result in borehole enlargement and the release of free gas into the borehole. This shift by all estimates, even when coring conditions stay inside the hydrate stability zone, shrinks the window between the estimated conditions and the hydrate stability boundary. This shift is likely to compromise the hydrate-bearing cores while they are being recovered from the bottom-hole to the rig floor. In this report we present two examples:

- 1) Assuming temperature and pressure from in-situ estimates:

Hydrate within the target reservoirs (Orange and Blue) at Walker Ridge Block 313 (WR 313) will be outside the hydrate stability zone in the presence of a drilling mud with 9.5 wt.% salinity (the salinity of the proposed 10.5 ppg salt-based mud) at in situ pressure and temperature. Thus, the hydrate will be unstable. A 10.5 ppg salt-based mud may result in dissociation of the hydrate into its components: water and gas. 10.5 ppg salt-based mud may enlarge the borehole, release free gas into the borehole, and compromise the cores.

- 2) Assuming temperatures equal to the measured LWD borehole temperatures at this location:

Hydrate within the target reservoirs will be stable with a salinity of 9.5 wt.% (the salinity of the proposed 10.5 ppg salt-based mud), but possibly unstable (just at the methane hydrate stability boundary) for a salinity of 17.2 wt.% (the salinity of the proposed 13.5 ppg salt-based kill mud). If the borehole has the same temperature as recorded during previous LWD drilling at this location. A 13.5 ppg salt-based kill mud may destabilize the borehole.

More importantly, a 10.5 ppg salt-based mud does not provide a large enough window between the estimated conditions and the hydrate stability boundary. Core temperatures and pressures fluctuate from the bottom-hole conditions as the core is brought up from the bottom-hole to the rig floor. These fluctuations are likely to cause the hydrate in the cores to touch or cross the stability boundary. Therefore, cores captured using a 10.5 ppg salt-based mud are likely to be compromised during core recovery to the rig floor.

## Contents

1.0	Executive Summary.....	1
2.0	Introduction .....	2
3.0	Background .....	3
	Previous referenced hydrate expeditions.....	3
	In-situ, borehole, and core temperatures .....	3
	In-situ and core chamber pressure .....	7
	Hydrate stability.....	7
4.0	Discussion.....	8
	Hydrate stability in the borehole during circulation.....	8
	Hydrate stability in the borehole when circulation stops.....	12
	Hydrate stability in the acquired core .....	13
5.0	Summary .....	15
6.0	References .....	16

## 2.0 Introduction

The drilling plan at WR 313 includes up to three coring holes. We will pressure core two deep primary hydrate reservoirs, several smaller hydrate-bearing sands, and intermittent background mud both above and below the primary targets. The primary targets are the Upper Blue and Orange hydrate-bearing sands. These sands dip toward the northwest from the proposed coring hole WR 313 F002 (TBONE-2A), through WR 313 H002 (TBONE-1B), to WR 313 G002 (TBONE-3B). The total depths of each proposed hole are 2,745 feet below seafloor (fbsf, 9119 feet below sea level (fbsl)), 3,010 fbsf (9470 fbsl), and 3085 fbsf (9652 fbsl), respectively. The water depths are 6374, 6460, and 6567 feet, respectively.

It is proposed that a salt-saturated, water-based mud might improve borehole stability relative to a fresh-water-based mud. The proposed plan is to bring a 16 ppg premixed salt-saturated mud on board and then dilute this to achieve a salt-based 10.5 ppg drilling mud and 13.0 ppg kill mud. The expected concentration of salt in the 10.5 ppg mud would be 9.5% NaCl (61,700 ppm of Cl / 40,100 ppm of Na. 35.21 ppb or 102,000 ppm of NaCl). The 13.0 ppg kill mud would dilute to 17.2% NaCl (118,000 ppm Cl / 77,000 ppm of Na. 68.47 ppb or 195,000 ppm of NaCl).

While a salt-based mud may promote borehole stability, it also may destabilize the hydrate, the recovery of which is the primary goal of our expedition. When drilling, the salt-based mud may destabilize the in situ hydrate, which will cause the hydrate to dissociate into water and gas, the sediment fabric to collapse, the borehole to widen, and possibly release free gas into the borehole. A second concern is that the hydrate-bearing cores will be captured with the salt-based mud inside the core chamber. If the drilling fluid is saline and the temperature swings during acquisition are similar to our previous expedition; the hydrate may become unstable. This would compromise the sample by causing hydrate in the core samples to dissociate into water and gas during retrieval before chilling on

the rig floor. This dissociation would cause the sediment fabric to collapse making the sample of limited use for core analysis.

## 3.0 Background

### Previous referenced hydrate expeditions

Two hydrate expeditions are referenced: the Gulf of Mexico Gas Hydrate Joint Industry Project Leg II (JIP II) and University of Texas Hydrate Pressure Coring Expedition (UT-GOM2-1).

Logging-while-drilling (LWD) was successfully accomplished at the WR 313 H and G, and the Green Canyon Block 955 (GC 955) H locations during JIP II. The borehole temperature and pressure profile were recorded during LWD operations (Collett et al., 2009; Collett et al., 2012). The expedition used a water-based mud system and drilled with seawater and 8.8 ppg gel sweeps to a depth of 8449 fbsl at WR 313 H (water depth of 6460 feet); below that depth the WR 313H was continuously drilled with a 10.5 ppg mud. The water depth was 6451 feet. They drilled with seawater above and 10 ppg mud below a depth of 9192 fbsl; and 10.5 ppg below 9547 fbsl at WR 313 G (Collett et al., 2009; Collett et al., 2012). The water depth was 6563 feet. The salinity of the 10.5 ppg mud was between tap water (equivalent to 1-100 mg/L Chlorides) and seawater (equivalent to 18,500 mg/L Chlorides). The time between commencement of drilling and plugging the hole, was ~1 day and ~2 days for the H and G holes, respectively. The flow rates during drilling were 380-410 gpm. The total depth was 9834 fbsl and 10,148 fbsl for the H and G holes, respectively (Collett et al., 2009). During drilling there was occasional pack-off at depths above 2629 fbsf (9192 fbsl) , related to issues with clearing drill cuttings when they first attempted to drill with seawater. They encountered no issues when they switched to a 10.5 ppg water-based mud at depths greater than 2985 fbsf (9548 fbsl) (Collett et al., 2009; Collett et al., 2012).

Hydrate pressure-coring was successfully accomplished GC 955 during the UT-GOM2-1 expedition. The expedition used a water-based mud system. Temperature and pressure measurements were recorded inside the pressure core chamber and on a wireline pulling tool. These measurements provide insight into the magnitude of temperature and pressure changes and were used to determine if the cores were compromised. The GC 955 H002 hole was drilled with seawater and gel sweeps to 1343 fbsf (8062 fbsl) and then with 10.5 ppg mud to total depth 1423 fbsf (8090 fbsl). The water depth was 6667 feet.

The GC 955 H005 well was drilled with seawater and gel sweeps to 1423 fbsf (8089 fbsl) and then with 9.5 ppg mud to 1443 fbsf (8109 fbsf), and then with 10.5 ppg mud to a total depth of 1475 fbsf (8141 fbsl) (Flemings et al., 2018b; Thomas et al., in press). The water depth was 6666 feet. The salinity of the 10.5 ppg mud was between fresh and seawater. The time between commencement of drilling (spudding the hole) and plugging the hole with cement was ~4 days and ~5 days for H002 and H005, respectively. The flow rate was 50-250 gpm during coring. No problems were encountered with borehole stability.

### In-situ, borehole, and core temperatures

Estimated in-situ, measured borehole, and measured coring temperatures for hydrate-bearing intervals of interest from WR 313 and GC 955 are shown in Table 1.

The in-situ temperatures at GC 955 and WR 313 (Table 1 E) are estimated from the interpreted depth of the bottom seismic reflection (BSR) using the assumptions of three phase equilibrium at the BSR, the seafloor water temperature, hydrostatic pressure, and pore water salinity equal to seawater salinity.

Table 1. Pressure and Temperature information for key WR 313 and GC 955 hydrate-bearing intervals A. Hole name, B. Interval in the hole, C. Top of the interval in fbsf, D. Base of the interval in fbsf, E. In-situ temperature. The in-situ formation temperature for WR 313 expedition was estimated using a seafloor temperature of 4 °C, and a temperature gradient of 6.0 °C/1000 ft (10.8 °F/1000 ft). The in-situ temperature for GC 955 location H was estimated to be 10.5 °C/1,000 ft (34.5 °C/km, or 18.9 °F/1,000 ft) F. Measured borehole temperatures from the JIP II LWD expedition (Collett et al., 2009). The LWD temperature has a precision of +/- 1.0 °C. G. Coring temperature measured at coring depth by Data Storage Tags (DSTs) placed in the core chamber. H. Coring recovery temperature measured at the rig floor after retrieval by Data Storage Tags (DSTs) placed in the core chamber. DSTs have an advertised accuracy of +/-0.1 °C (0.18 °F) and a precision of 0.032 °C (0.058 °F). I. Calculated hydrostatic pressure. WR 313 used a pressure gradient of 0.465 psi/ft and GC 955 a pressure gradient of 0.447 psi./ft., J. Core Recovery pressure measured by a pressure gauge on the rig floor after retrieval.

A	B	C	D	E	F	G	H	I	J
Hole	Sand /Core	Top FBSF	Base FBSF	In-situ temperature °C	LWD borehole temperature °C	Coring temperature s °C	Core recovery temperature °C	In-situ pressure MPa	Core recovery pressure MPa
WR 313 H002	Upper Blue Sand	2187	2263	17.1-17.6	8.9	-	-	27.7-28.0	-
WR 313 H002	Orange sand	2649.9	2693.9	19.9-20.2	10.6	-	-	29.2-29.3	-
WR 313 G002	Upper Blue sand	2714.4	2787.4	20.3-20.7	12.5	-	-	29.8-30.0	-
WR 313 G002	Kiwi sand	3051.4	3072.4	22.3-22.4	14.0	-	-	30.8-30.9	-
GC 955 H005	Hydrate-bearing cores	1368	1475	18.4-19.4	7.0	6.4-10.0	8.1-19.5	24.7-25.1	12.3-24.0

The LWD borehole temperatures were measured during the JIP II expedition (Collett et al., 2009). Coring temperatures were measured by Data Storage Tags (DSTs) placed inside the core chamber during the UT-GOM2-1 expedition.

Temperatures measured during coring at GC 955 (Table 1 G) are approximately equal the LWD borehole temperatures at GC 955 (Table 1 F). A detailed example of the core temperature history for GC 955 core H005-05FB, is shown in Figure 1. Wireline tension and depth, flow rate, coring tool rate of penetration and weight-on-bit histories (Figure 1 A and C), were used to identify the timestamps of each coring step. The timestamps were then used to find the correlating core temperature and pressure measurements for each step.

The core temperature during coring for H005-05FB (Figure 1 B, dotted blue line, between steps 3 and 4) was 9.15-9.45 °C. The temperature was slightly higher than the borehole temperature of 7 °C from the JIP II GC 955 H LWD data at the depth that core H005-05FB was taken (Figure 1 B, lower light blue line). The coring temperature was much lower than the in-situ estimate of 18.6 °C (Figure 1 B, upper light blue line).

Temperatures during coring varied from coring run to coring run. Temperatures for all 11 cores that sealed in Hole GC 955 H005 in the hydrate-bearing sand, varied from 6.5-10.0 °C (Table 1 G). These temperatures overlap the LWD measured temperature within the cored interval of 7 °C.

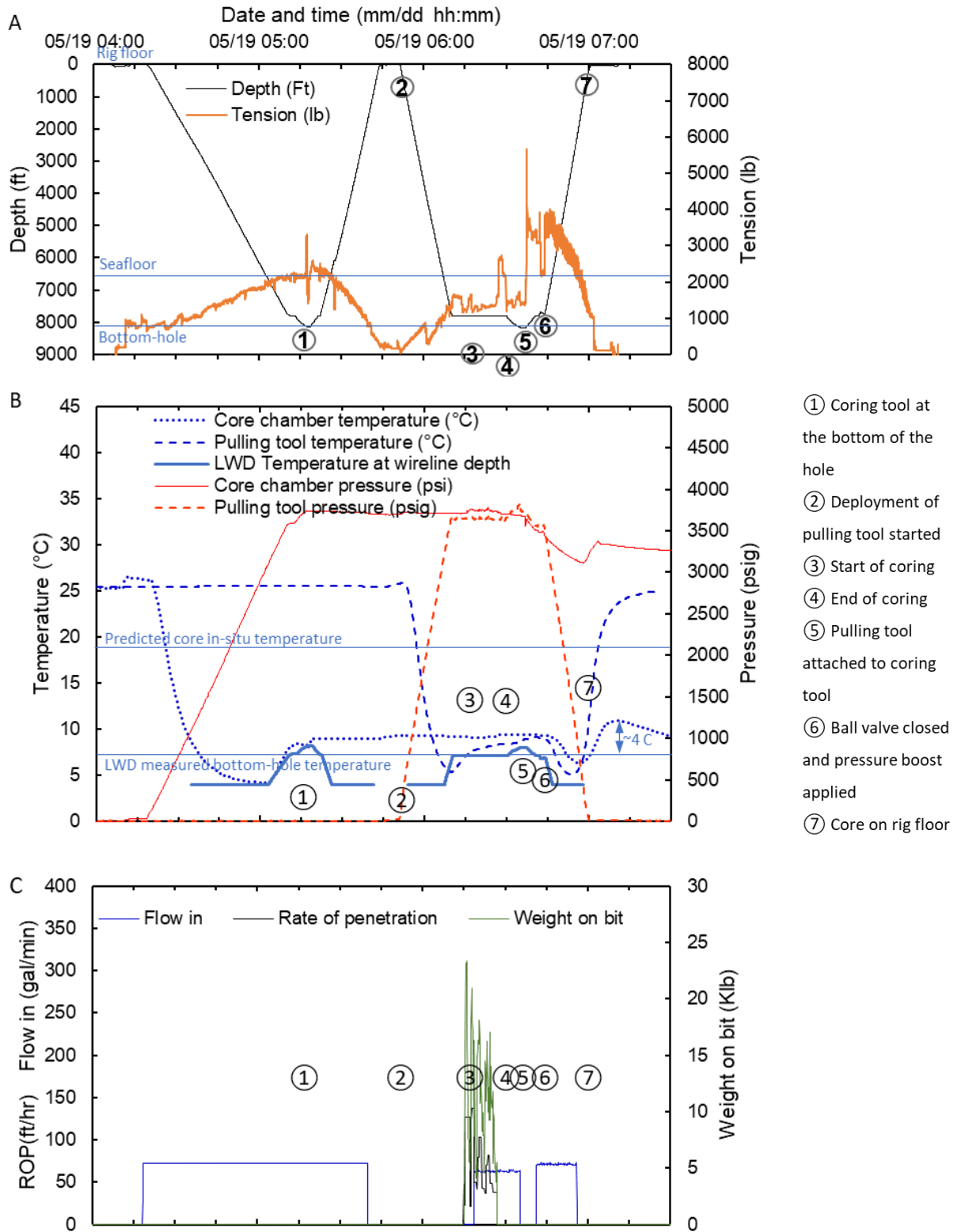


Figure 1. Tension, depth, temperature, pressure, flow rate, rate of penetration, weight on bit history for coring run GC 955 H005-05FB. A. Tension (in orange) and Depth (in black) with time. B. Coring chamber temperature (dotted blue line), Pulling tool temperatures (dashed blue line), borehole temperature (LWD temperature) at wireline depth

when wireline is below 2000 fbsl (solid blue line), core chamber pressure (red line), pulling tool pressure (dashed red line) with time. C. Flow in (blue line), rate of penetration (black line), and weight on bit (green line) with time. The solid blue line represents the temperature of the fluid around the wireline. The coring chamber and the pulling tool temperatures should follow the borehole temperature if the wireline speed is slow enough for temperatures to equilibrate.

Points 0-> 1: the coring tool is deployed at the rig floor (25.5 °C, 77.9 °F) while drilling fluid is being circulated. The temperature inside the core chamber drops as it is lowered through the water column until it reaches the seafloor (4.2 °C, 39.6 °F, journey is 45 minutes). The temperature then rises below the seafloor until it reaches coring depth (bottom-hole, 9.0 °C, 48.2 °F) at Point 1. The wireline drop rate is slow and the coring chamber is open to the borehole. The coring chamber temperature has time to equilibrate to the borehole and the core chamber temperature (dotted blue line) changes as the borehole temperature (solid blue line) changes.

Points 1 -> 2: The coring chamber sits at the bottom of the hole while the wireline is pulled up. Circulation is stopped when the hook reaches the rig floor so a latching tool can be replaced with the pulling tool.

Point 2-> 3: The pulling tool is deployed on the wireline without circulation while the coring tool is at the bottom of the hole. The pulling tool temperature (dashed blue line) drops as it is lowered through the water column until it just passes the seafloor (5.4 °C, 41.7 °F, journey is 16 minutes). The temperature then rises below the seafloor until it stopped about 350 ft above the coring tool at , 8.0 °C, 46.4 °F). The drop rate of the pulling tool is fast. The pulling tool temperature does not have time to equilibrate with the borehole. The pulling tool temperature (dashed blue line) rises more slowly than the borehole temperature (solid blue line). Coring begins. The temperature inside the coring chamber increases only from 8.95 to 9.04 °C from point 2 to 3.

Points 3-> 4: The temperature inside the core chamber and the pulling tool temperature rise very slightly. Points 4->5: The pulling tool is lowered to latch into the coring tool. The temperature rises as it is lowered.

Points 5->6: the coring tool is pulled up triggering ball valve closure (See Thomas et al. in press for details) to about 350 ft above coring depth and stays there for about a minute. The temperature of the pulling tool drops at a faster rate than the coring chamber but not as fast as the borehole temperature. The temperature of the core chamber, now filled with the hydrate-bearing core and closed off from the circulating drilling fluid, barely starts to drop. The chamber has not yet sealed and the pressure in the chamber drops with the borehole pressure (as indicated by the pulling tool pressure measurement).

Points 6->7: Pulling of the coring tool resumes. The pulling tool temperature drops and rise as the temperature in the water column, reaching the rig floor temperature. The pulling tool pressure drops to atmospheric. The core chamber seals sometime before or as pulling reinitiates. The chamber pressure continues drops and rises with the chamber temperature after sealing. The measured pressure at the rig floor is 2.5 MPa lower than the in-situ pressure of 24.8 MPa . The maximum chamber temperature is 10.9 °C, (51.6 °F), which is ~4 °C (~7 °F) above the measured LWD borehole temperature.

Core temperatures fluctuate during recovery, getting colder as the core is pulled up from the bottom-hole to the seafloor and through the cold deep water, and getting warmer as the core is pulled up through the shallow water and into the air (Figure 1, dotted blue line, between steps 4 and 7). The core recovery temperature (Table 1 H) is defined as highest temperature the core reaches during recovery. The core recovery temperature for H005-05FB was 10.93 °C. For all cores that sealed from Hole GC 955 H005, the core recovery temperature was 8.1 to 19.5 °C. Removing two cores (H005-04FB, -07FB) with unexplained unusually high temperature increases (Flemings et al., 2018a; Thomas et al., in press), the average recovery temperature was 10.64 °C and the average increase over the lowest temperature measured after coring was 4.6 °C. Because we will use a similar rate to pull up the core, we assume that the WR 313 core temperature will decrease from its coring temperature with a similar rate as at GC 955.

Because the water depths are similar, we assume that the WR 313 core temperatures will increase from its lowest point by an average of 4.6 °C for WR 313.

### In-situ and core chamber pressure

The in-situ formation pressure at WR 313 is assumed to be hydrostatic and is approximated assuming a pressure gradient of 3.21 MPa/1,000 ft (0.465 psi/ft). The in-situ formation pressure estimate for GC-955 using a pressure gradient of 3.08 MPa/1,000 ft (0.447 psi/ft).

Core is often captured below the in situ pressure (Flemings et al., 2018c; Thomas et al., in press). A small amount of pressure will always be lost due to expansion of the pressure chamber volume during ball valve closure. However, addition pressure may be lost if the core chamber does not seal right away. The recovery pressure of H005-05FB was 22.3 MPa, 2.5 MPa lower than the in-situ pressure of 24.8 MPa. Six of eleven pressure cores from GC 955 H005 hydrate-bearing sand that sealed, sealed at pressures 2.8-12.4 MPa (400-1800 psi) below in situ (Thomas et al., in press). Two additional cores lost even more pressure before a pressure boost was applied at the rig floor. The typical pressure drop for GC 955 was 3.2 MPa. After sealing, the pressure will also swing as the core chamber temperature swings.

### Hydrate stability

Whether the hydrate destabilizes depends on the pressure, temperature and salinity conditions. Figure 2. shows the stability zones and boundaries versus pressure and temperature for four different drilling fluids: fresh water (0 wt.% NaCl, dotted green line), seawater (3.5 wt.% NaCl, dotted blue line, the assumed in-situ salinity), 10.5 ppg salt-based mud (9.5 wt.% NaCl, dotted orange line) and 13.0 ppg salt-based mud (17.2 wt.% NaCl, dotted red line). Similar to ice, adding salt shifts the melting point of the hydrate to lower temperatures. In Figure 2, hydrate is stable to the left of the phase boundary, at lower temperatures, and unstable to the right of the phase boundary, at higher temperature. The solid light and dark blue, orange, and green lines in Figure 2, show our best estimates of the in-situ pressure and temperature condition for our hydrate reservoirs at WR 313. The solid grey line in Figure 2, show our best estimate of the in-situ pressure and temperature condition for the hydrate-bearing sands cored at GC 955. The higher temperatures of the deeper WR 313 hydrates place them much closer to the hydrate stability boundary than at GC 955.

The estimated H002 in-situ temperature of the Orange and Blue sands are currently within, and stay within, the hydrate stability zone (to the left of the boundary), when using NaCl concentrations for fresh (0 wt.% NaCl), but fall outside the hydrate stability zone (to the right of the boundary) for 9.5 % (H002 Orange and G002 sands) and 17.2% NaCl (H002 Orange sands). The solid dark blue and dark orange lines (Figure 2) show our best estimate of the borehole conditions from JIP II LWD data for each sand. The estimated borehole temperatures of the Orange and Blue reservoirs are currently within, and stay within, the hydrate stability zone (to the left of the boundary), when using NaCl concentrations for fresh to 10.5 ppg salt-based mud (9.5 wt.% NaCl).

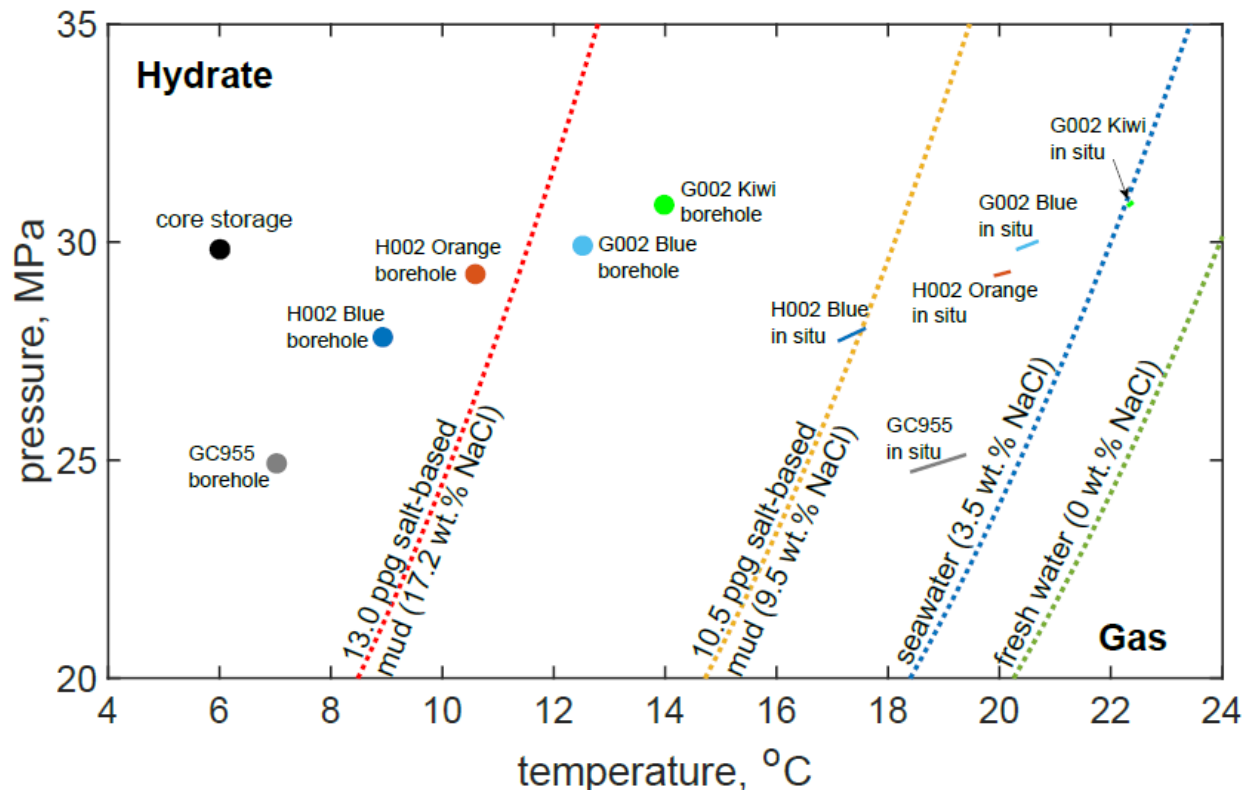


Figure 2. Methane hydrate phase diagram for different salinities. The dotted green, blue, orange and red lines are the methane hydrate phase boundaries for fresh water (0 wt.% NaCl), seawater (3.5 wt.% NaCl, the assumed in-situ salinity), 10.5 ppg salt-based mud (9.5 wt.% NaCl) and 13.0 ppg salt-based mud (17.2 wt.% NaCl), respectively. Methane hydrate is stable to the left of the phase boundary and unstable to the right. The solid light blue and orange lines are the in situ conditions for the H002 Blue and Orange sands, respectively. We used the temperature LWD borehole temperature to estimate the coring borehole temperature. The pressure gradient is 0.465 psi/ft. The solid dots are the estimated borehole temperatures and pressures while coring for each sand. The hydrate phase boundaries are calculated by the models presented in Liu and Flemings (2007). The black dot shows the expected pressure and temperature conditions for off-shore core storage of 6 °C (42.8 °F) and 30 MPa (4351 psi).

## 4.0 Discussion

### Hydrate stability in the borehole during circulation

To understand the risk of hydrate dissociation within the borehole with the use of a 10.5 ppg or higher salt-based mud, we look at the estimated conditions of our target hydrate-bearing reservoirs with depth. The estimated in-situ temperature, the borehole temperature from LWD drilling, the hydrate stability boundaries, and the base of hydrate stability are plotted with depth for WR 313 H002 (Figure 3).

Assuming temperature and pressure from in-situ estimates

The in situ temperature (Figure 3, solid black line) increases with increasing depth and the location of the Blue sand (aqua blue highlight on the black line) and Orange sand (dark orange highlight on the black line) are shown on the temperature line. The pure methane hydrate phase boundary for NaCl concentrations of fresh water (0 wt.% NaCl, solid green line), seawater (3.5 wt.% NaCl, solid

blue line), 10.5 ppg salt-based mud (9.5 wt.% NaCl, solid orange line) and 13.0 ppg salt-based mud (17.2 wt.% NaCl, solid red line) as a function of depth and temperature are also shown. The depth at which hydrate becomes unstable, or the base of hydrate stability zone (BHSZ), for each salt concentration is determined by finding the depth where the methane hydrate stability boundary and the in-situ temperature cross (for the assumed hydrostatic pore pressure). For example, the natural BHSZ for the in-situ salinity of 3.5 wt.% NaCl at H002, shown by the dashed blue line (Figure 3) (9395 ft below sea level) is located at the depth where the in-situ temperature (solid black line) intersects the methane hydrate phase boundary with 3.5 wt.% NaCl (solid blue line). If NaCl concentration of 9.5 wt.% and 17.2 wt.% are used in H002, the BHSZ moves up by 768 ft (from where the blue line crosses to where the orange line crosses the solid black line) and 2044 ft (from where the blue line crosses to where the red line crosses the solid black line), respectively. With 10.5 ppg (9.5 wt.% NaCl) drilling fluid, the Blue and Orange reservoirs are outside of hydrate stability zone (to the right of the 10.5 ppg (9.5 wt.% NaCl) hydrate stability phase boundary and below the 10.5 ppg BHSZ), at in situ conditions. Thus, for our best estimate of in situ conditions, we show that in H002 a 10.5 ppg mud (9.5 wt.% NaCl) and a 13.0 ppg kill mud 17.2 wt.% NaCl) will result in hydrate instability for both the Orange and the Blue reservoirs. In fact, this is a worst case scenario. This will result in dissociation of the hydrate into its components: water and gas.

Assuming temperatures equal to the measured LWD borehole temperatures at this location The borehole temperature is based on a fit of the observed temperatures during drilling of the JIP LWD H001 well (Figure 3, dashed black line) from the seafloor to the BHSZ. It also increases with increasing depth, but the gradient is lower. With 10.5 ppg (9.5 wt.% NaCl) drilling fluid and 13.0 ppg (17.2 wt.% NaCl) drilling fluid, the estimated borehole temperature is now inside the hydrate stability zone (to the left of the 10.5 ppg (9.5 wt.% NaCl) and 13.0 ppg (17.2 wt.% NaCl) hydrate stability phase boundaries and above the 10.5 ppg and 13.0 ppg BHSZ (not shown)). Thus, for our best estimate of coring conditions, the H002 Blue and Orange reservoirs would remain hydrate stable with 10.5 ppg salt-based mud (9.5 wt.% NaCl) and 13.0 ppg salt-based mud (17.2 wt.% NaCl).

A similar analysis of the in-situ and borehole temperature versus the hydrate stability boundaries was pursued in Figures 4 and 5 for the shallower F002 and deeper G002 holes. The F002 Blue and Orange reservoirs would remain hydrate stable with 10.5 ppg salt-based mud (9.5 wt.% NaCl) and 13.0 ppg salt-based mud (17.2 wt.% NaCl).

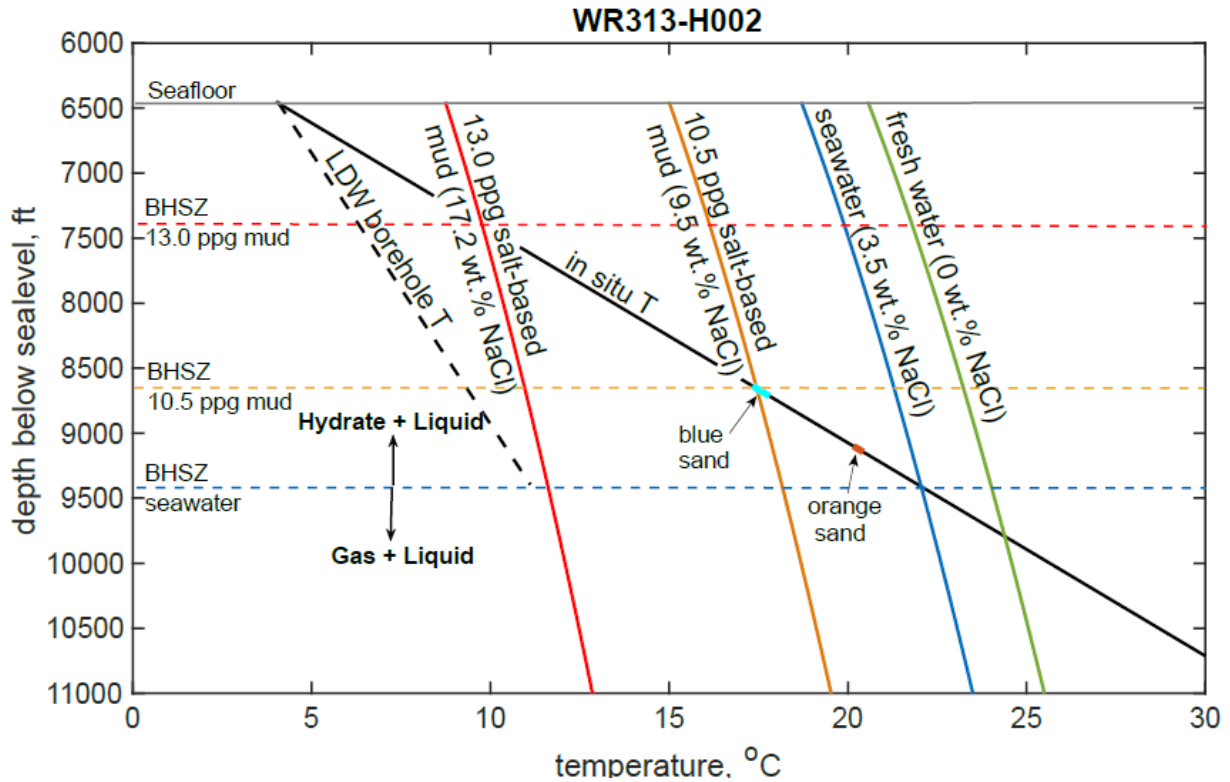


Figure 3. WR313-H002 estimated borehole conditions versus hydrate stability with different drilling fluids. The solid black line shows the predicted in situ reservoir temperature distribution with depth at WR313-H002, the main coring hole. The dashed black line shows the fit of the observed LWD borehole temperature. The corresponding pure methane hydrate phase boundary for seawater (0 wt.% NaCl, solid green line), seawater (3.5 wt.% NaCl, solid blue line, assumed in situ salinity), 10.5 ppg salt-based mud (9.5 wt.% NaCl, solid orange line), and 13.0 ppg salt-based mud (17.2 wt.% NaCl, solid redline). The natural base of hydrate stability zone (BHSZ, dashed blue line, 9395 ft below sea level) is located at the depth where the in situ temperature (solid black line) intersects the methane hydrate phase boundary for seawater, the assumed in situ salinity of 3.5 wt.% NaCl (solid blue line). The solid grey line represents seafloor depth (6460 ft below sea level). When 10.5 ppg (9.5 wt.%) and 13.0 ppg (17.2 wt.% NaCl) drilling muds are used, and when the temperature equals in situ temperature (solid black line), the BHSZ is moved up by 768 ft (from where the blue line intersects to where the orange line intersects the solid black line) and 2044 ft (from where the blue line intersects to where the red line intersects the solid black line), respectively. The addition of salt moves the Orange and Blue sand out of the hydrate stability zone. The methane hydrate becomes unstable and will melt into water and methane. However, if the borehole temperature follows the dashed black line, hydrate in both Blue and Orange sand stay stays stable when both drilling muds are used.

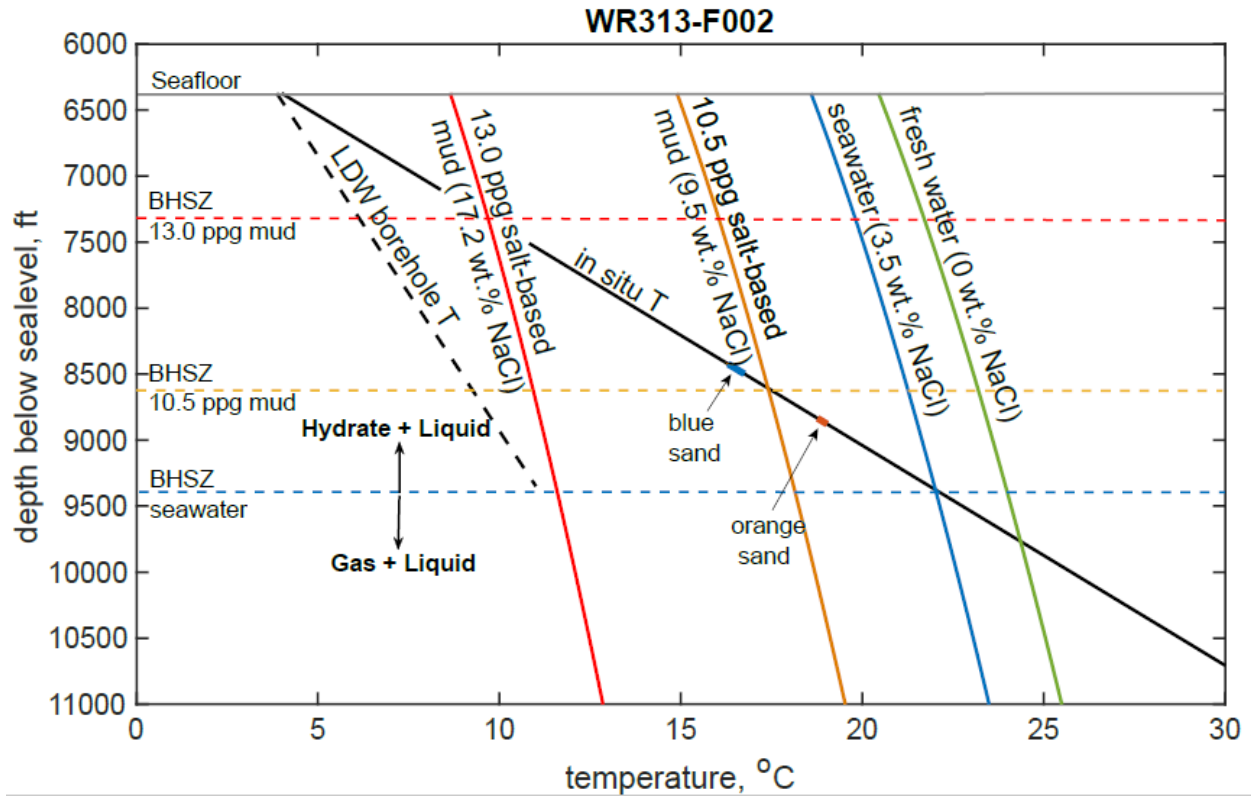


Figure 4. WR313-F002 estimated borehole conditions versus hydrate stability with different drilling fluids. The solid black line shows the predicted in situ reservoir temperature distribution with depth at WR 313 F002, the shallower coring hole. The dashed black line shows the fit of the observed LWD borehole temperature. The corresponding pure methane hydrate phase boundary for seawater (0 wt.% NaCl, solid green line), seawater (3.5 wt.% NaCl, solid blue line, assumed in situ salinity), 10.5 ppg salt-based mud (9.5 wt.% NaCl, solid orange line), and 13.0 ppg salt-based mud (17.2 wt.% NaCl, solid redline). The natural base of hydrate stability zone (BHSZ, dashed blue line, 9367 ft below sea level) is located at the depth where the in situ temperature (solid black line) intersects the methane hydrate phase boundary for seawater (the assumed in situ salinity, 3.5 wt.% NaCl, solid blue line). The solid grey line represents seafloor depth (6374 ft below sea level). When 10.5 ppg (9.5 wt.%) and 13.0 ppg (17.2 wt.% NaCl) drilling muds are used, and when the temperature equals in situ temperature (solid black line), the BHSZ is moved up by 780 ft (from where the blue line crosses to where the orange line crosses the solid black line) and 2098 ft (from where the blue line crosses to where the red line crosses the solid black line), respectively. The addition of salt moves the Orange sand and Orange and Blue sand out of the hydrate stability zone. The methane hydrate becomes unstable and will melt into water and methane. However, if the borehole temperature follows the dashed black line, hydrate in both the Blue and Orange sand stays stable when both drilling muds are used.

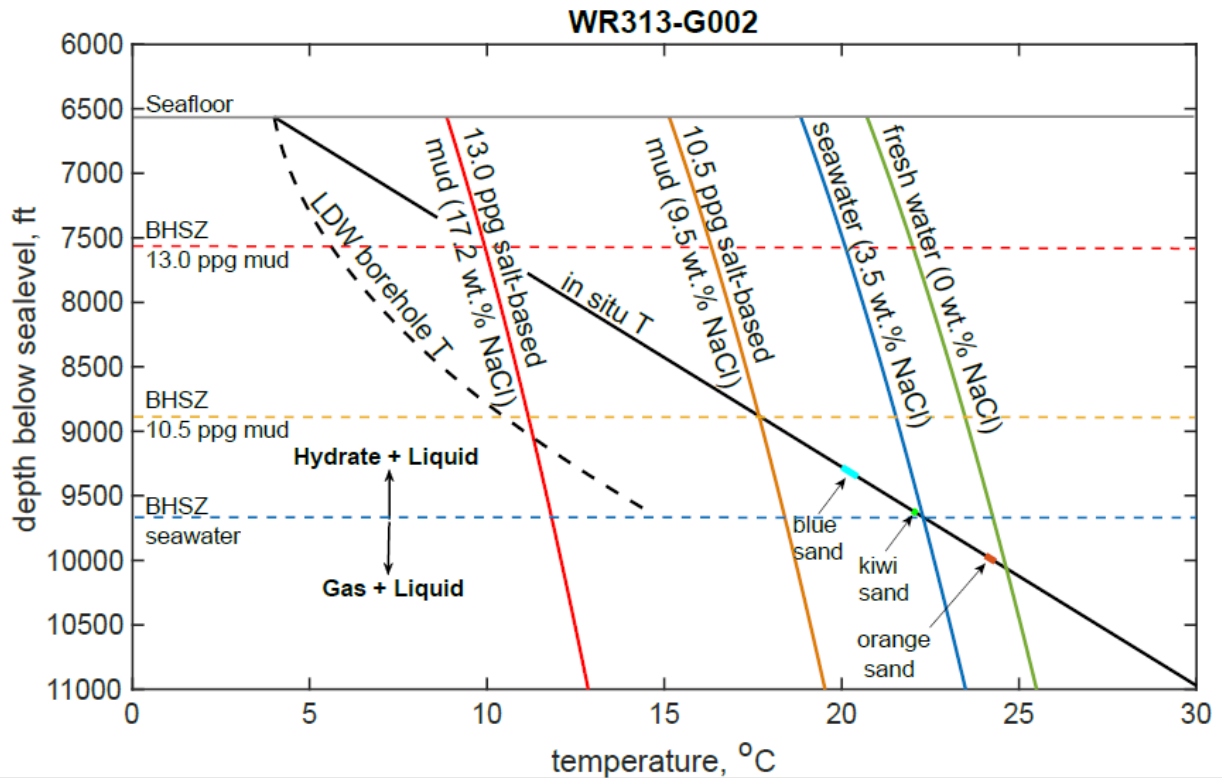


Figure 5. WR313-G002 estimated borehole conditions versus hydrate stability with different drilling fluids. The solid black line shows the predicted in situ reservoir temperature distribution with depth at WR313-G002, the main coring hole. The dashed black line shows the fit of the observed LWD borehole temperature. The corresponding pure methane hydrate phase boundary for seawater (0 wt.% NaCl, solid green line), seawater (3.5 wt.% NaCl, solid blue line, assumed in situ salinity), 10.5 ppg salt-based mud (9.5 wt.% NaCl, solid orange line), and 13.0 ppg salt-based mud (17.2 wt.% NaCl, solid redline). The natural base of hydrate stability zone (BHSZ, dashed blue line, 9667 ft below sea level) is located at the depth where the in situ temperature (solid black line) intersects the methane hydrate phase boundary for the assumed in situ salinity of 3.5 wt.% NaCl (solid blue line). The solid grey line represents seafloor depth (6567 ft below sea level). When 10.5 ppg (9.5 wt.%) and 13.0 ppg (17.2 wt.% NaCl) drilling muds are used, and when the temperature equals in situ temperature (solid black line), the BHSZ is moved up by 809 ft (from where the blue line crosses to where the orange line crosses the solid black line) and 2137 ft (from where the blue line crosses to where the red line crosses the solid black line), respectively. The addition of salt moves the Orange and Blue sand out of the hydrate stability zone. The methane hydrate becomes unstable and will melt into water and methane. However, if the borehole temperature follows the dashed black line, hydrate in both Blue and Orange sand stay stable when 10.5 ppg drilling muds (9.5 wt.% NaCl) is used, and become unstable when 13.0 ppg salt-based mud (17.2 wt.% NaCl) is used.

### Hydrate stability in the borehole when circulation stops

The UT-GOM2-1 DST data also provides some insight into the rate of heat transfer from the formation to the borehole during periods of non-circulation. During coring run H005-05FB, the flow rate was stopped for 39 min (Figure 1 C, shown in blue, 2017 May 18 0540 to 0618) in order to swap the latching and pulling wire line tools. During this time there was no significant increase in temperature (temperatures were slowly rising during the period surround no flow from 8.95 to 9.04 °C (48.1 to 48.3 °F), 2017 May 18 0512 to 0642, when the flow rate was 75 gpm).

## Hydrate stability in the acquired core

To successfully acquire uncompromised hydrate-bearing sediment cores, the cores must stay within the hydrate stability zone. Hydrate captured at unstable conditions will dissociate into gas and water, the sediment fabric will collapse, and the core degrade until they are placed in a 6 °C (42.8 °F) chiller bath, and a pressure boost is applied (as needed).

To successfully acquire uncompromised hydrate-bearing sediment cores, coring conditions must also be well away from the hydrate stability boundary. This window between the coring conditions and the hydrate stability boundary is necessary to provide room for core temperature and pressure fluctuations as the core is brought from the bottom of the hole to the rig floor. Core captured close to the stability boundary may also dissociate depending on these pressure and temperature fluctuations. The amount of dissociation will depend on how long the core are outside of the hydrate stability zone and how far their conditions are from the stability boundary. At GC 955 this window was large. Still, a number of cores touched and may have crossed the stability boundary. In the two worst cases, a UT-GOM2-1 pressure core that destabilized during recovery for ~8 mins fortunately did not show degradation, but a second core that was destabilized for ~80 min was severely compromised (Thomas et al., in press).

The window, between the coring conditions and the hydrate stability boundary, at WR 313 using a 10.5 ppg salt-based mud (9.5 wt.% NaCl), is much smaller than for GC 955. This is especially true for the deep hydrate-bearing sands in G002. To illustrate the impact of this smaller window on core quality for this expedition, we adjusted the temperature and pressure history of H005-05FB, to possibly reflect a coring run for the WR 313 H Orange sand.

The coring temperatures at WR 313 were assumed to be the same to slightly higher than the measured borehole temperatures (Table 1 F) from the JIP II LWD expedition.

Core will cool from coring depth to the seafloor and as they pass through the colder sea depths. Cores will warm as they pass through the shallower sea depth and rise to the rig floor. Because the core pulling rate is fast and the same as GC 955, we assume that core chamber temperatures will not equilibrate with the borehole but will have a similar cooling rate as GC 955. Because the WR 313 sands are deeper, the magnitude of the cooling is assumed to be slightly larger. Because the water depth at WR 313 is similar to GC 955, we also assume that core warming, from the warmer shallower water and air temps at the rig floor, will have a similar magnitude during this expedition as at GC 955.

The assumed conditions for the WR 313 H Orange sand were: a capture temperature of 11.6 °C (the JIP II LWD borehole temp for the orange sand of 10.6 °C (51.1 °F) plus 1 °C); a temperature drop with the same rate as H005-05FB; a temperature rise during recovery with the same average magnitude as H005, 4.6 °C; and a sealed pressure of 25 MPa (4 MPa (725 psi) below in situ pressure of 29 MPa). Figure 6 A shows the DST temperature for UT-GOM2-1 H005-05FB in blue and the estimated WR 313 temperature for the H002 Orange sand in orange. Figure 6 B shows the DST pressure and temperature history for UT-GOM2-1 H005-05FB and the estimated history for WR 313 Orange sand using blue and orange circles respectively.

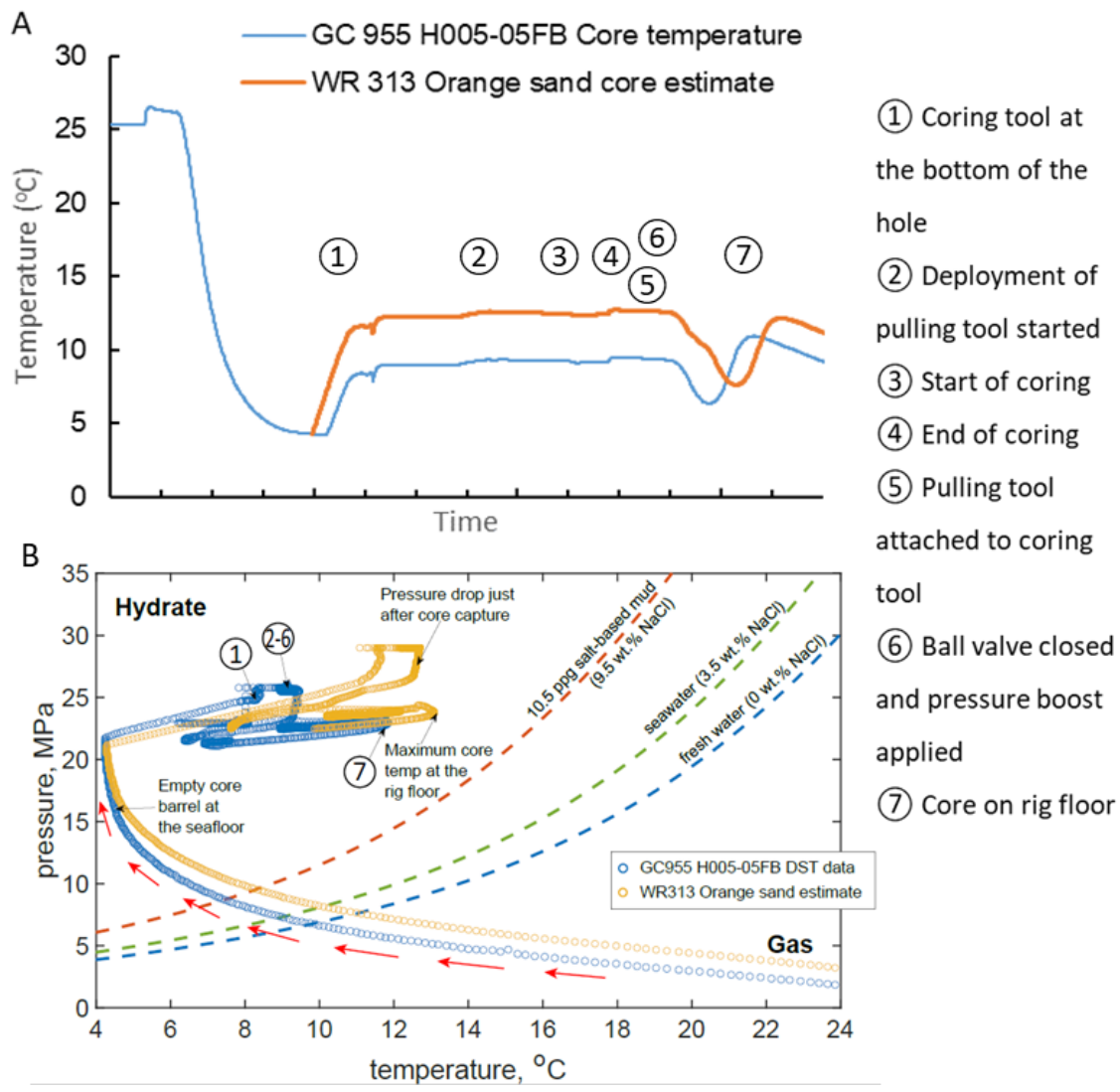


Figure 6. Estimated temperature and pressure swings during recovery vs. the hydrate stability boundary. A. The data storage tag (DST) temperature history for UT-GOM2-1 H005-05FB is shown in blue and the estimated temperature path for WR 313 Orange sand is shown in orange. Point 1. Since the Orange sand (orange) is deeper than the GC 955 sand (blue), the orange sand core temperature is assumed to continue to rise to just above the borehole temperature. Points 5-7. Since the Orange sand (orange) is deeper than the GC 955 sand (blue) it will take longer to climb to the seafloor. More cooling is assumed for the Orange sand core during this time, but at the same rate. The sea depth is almost the same at WR 313 and GC 955. The temperature cooling and rise of the Orange sand core from the seafloor to the rig should be about the same as the GC 955 core. B. The data storage tag (DST) pressure and temperature history for UT-GOM2-1 H005-05FB is shown in blue circles and the estimated pressure and temperature path for WR 313 Orange sand is shown in orange circles. The methane hydrate stability boundary for fresh water (0% NaCl, dashed blue line), seawater (3.5% NaCl, dashed green line), 10.5 ppg salt-based mud (9.5 wt.% NaCl, dashed orange line) are shown for comparison. Red arrows indicate increasing time. The estimated pressure and temperature swings during core recovery place the core much closer to and possible over the hydrate stability boundary for a 10.5 ppg salt-based mud. The assumed WR 313 Orange sand conditions used were a capture temperature of 11.6 °C (the JIP II LWD borehole temp for the orange sand plus 1 °C), temperature swing rates like GC 955 H005-05FB during recovery, and a sealed pressure of 25 MPa (3 MPa (725 psi) below in situ).

Figure 6 B also compares the estimated history against the stability boundary for fresh water (0 wt.% NaCl, dashed blue line), seawater (3.5 wt.% NaCl, dashed green line), and 10.5 ppg salt-based (9.5 wt.% NaCl, dashed orange line) mud. As shown, the higher borehole temperature estimates and estimated fluctuations place the core at pressure and temperature conditions closer to the hydrate stability boundaries. This combined with the smaller window for WR 313, creates a much higher chance for hydrate dissociation within the core during recovery at WR 313. Cores from the deeper G002 sands and cores with very late sealing or large temperature rises, such as the more extreme cases for GC 955 H005, would touch or cross the hydrate stability boundary and be very vulnerable to hydrate dissociation. If the cores at WR 313 were to show a smaller amount of cooling from coring depth to the seafloor, similar to GC 955, the cores would also be very likely to touch the hydrate stability boundary as they warm before reaching the rig floor during every coring run.

## 5.0 Summary

The primary objective for UT-GOM2-2 is to safely and successfully acquire uncompromised hydrate-bearing sediment cores. This can only be done if conditions stay within the hydrate stability zone, and well away from the hydrate stability boundary. Figure 7 shows a modified version of Figure 2 comparing the different pressure and temperature windows for GC 944 and WR 313. It is proposed that a salt-saturated, water-based mud might improve borehole stability for UT-GOM2-2 relative to a fresh-water-based mud. However, the window for WR 313 is already much smaller than GC 955 because the target sands at WR 313 are much deeper, and the addition of salt, shifts the hydrate stability boundary even closer to estimated conditions. This shift, by some estimates of pressure and temperature, where conditions now fall outside of the hydrate stability zone, may result in borehole enlargement and the release of free gas into the borehole. This shift by all estimates, even when coring conditions stay inside the hydrate stability zone, shrinks the window between the estimated conditions and the hydrate stability boundary. This shift is likely to compromise the hydrate-bearing cores while they are being recovered from the bottom-hole to the rig floor. Two assumptions of the coring conditions were presented:

- 1) Assuming temperature and pressure from in-situ estimates:

Hydrate within the target reservoirs (Orange and Blue) at Walker Ridge Block 313 (WR 313) will be outside the hydrate stability zone in the presence of a drilling mud with 9.5 wt.% salinity (the salinity of the proposed 10.5 ppg salt-based mud) at in situ pressure and temperature. Thus, the hydrate will be unstable. A 10.5 ppg salt-based mud may result in dissociation of the hydrate into its components: water and gas. 10.5 ppg salt-based mud may enlarge the borehole, release free gas into the borehole, and compromise the cores.

- 2) Assuming temperatures equal to the measured LWD borehole temperatures at this location:

Comparison of the LWD borehole temperature measurements at GC 955 to coring chamber and wireline temperatures at GC 955 show that the LWD borehole temperature is a reasonable estimate of the temperature encountered during coring. Hydrate within the target reservoirs will be stable with a salinity of 9.5 wt.% (the salinity of the proposed 10.5 ppg salt-based mud), but possibly unstable (just at the methane hydrate stability boundary) for a salinity of 17.2 wt.% (the salinity of the proposed 13.5 ppg salt-based kill mud). If the borehole has the same temperature as recorded during previous LWD drilling at this location. A 13.5 ppg salt-based kill mud may destabilize the borehole.

More importantly, a 10.5 ppg salt-based mud does not provide a large enough window between the estimated conditions and the hydrate stability boundary. Core temperatures and pressures fluctuate from the bottom-hole conditions as the core is brought up from the bottom-hole to the rig floor. These fluctuations are likely to cause the hydrate in the cores to touch or cross the stability boundary. Therefore, cores captured using a 10.5 ppg salt-based mud are likely to be compromised during core recovery to the rig floor.

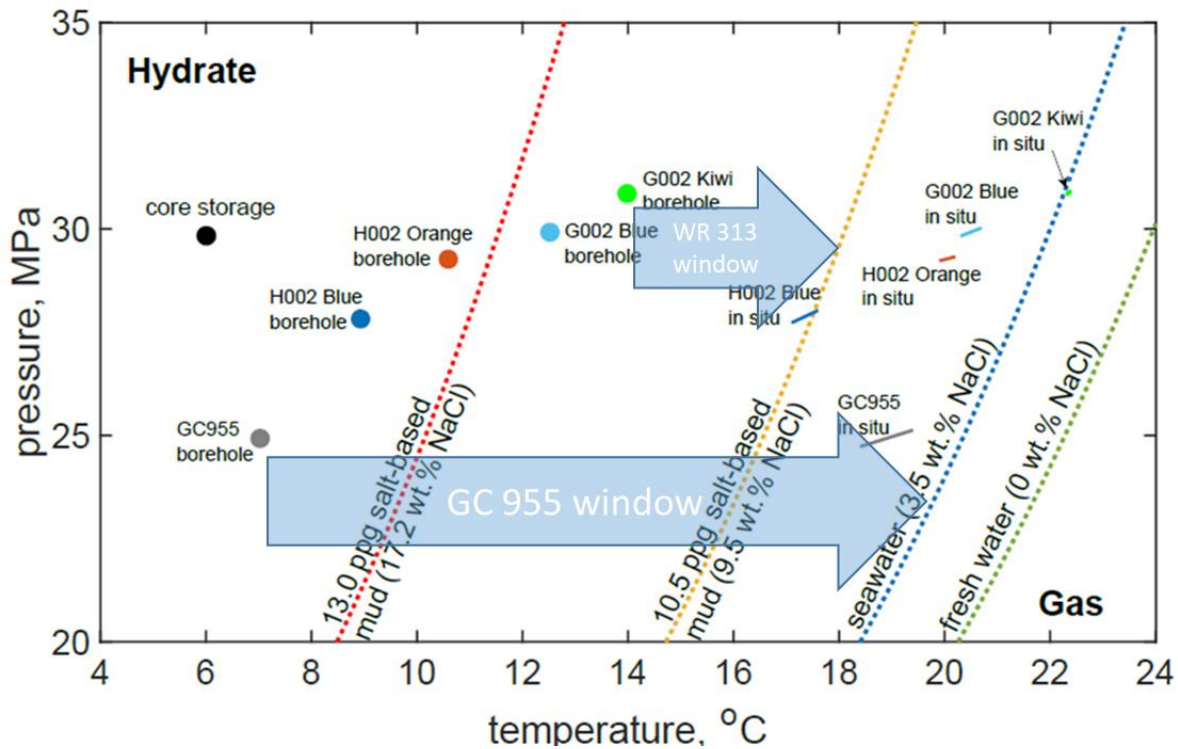


Figure 7. Repeat of Figure 2 highlighting the different pressure and temperature windows for hydrate recovery at GC 955 with a water-based mud and WR 313 with a 10.5 ppg salt-based mud.

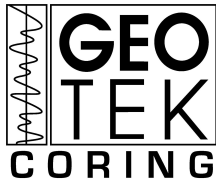
## 6.0 References

- Collett, T. S., R. Boswell, M. Frye, W. Shedd, P. Godfriaux, R. Dufrene, D. McConnell, S. Mrozewski, G. Guerin, A. Cook, E. Jones, and R. Roy, 2009, Gulf of Mexico Gas Hydrate Joint Industry Project Leg II: Operational Summary, Proceedings of the Drilling and Scientific Results of the 2009 Gulf of Mexico Gas Hydrate Joint Industry Project Leg II, p. 27.
- Collett, T. S., M. W. Lee, M. V. Zyrianova, S. A. Mrozewski, G. Guerin, A. E. Cook, and D. S. Goldberg, 2012, Gulf of Mexico Gas Hydrate Joint Industry Project Leg II logging-while-drilling data acquisition and analysis: Marine and Petroleum Geology, v. 34, p. 41-61.
- Flemings, P. B., S. C. Phillips, T. Collett, A. Cook, R. Boswell, and U.-G.-E. Scientists, 2018a, UT-GOM2-1 Hydrate Pressure Coring Expedition Hole GC 955 H005, in P. B. Flemings, S. C. Phillips, T. Collett, A. Cook, R. Boswell, and U.-G.-E. Scientists, eds., UT-GOM2-1 Hydrate Pressure Coring Expedition Report, Austin, TX, University of Texas Institute for Geophysics.

- Flemings, P. B., S. C. Phillips, T. Collett, A. Cook, R. Boswell, and U.-G.-E. Scientists, 2018b, UT-GOM2-1 Hydrate Pressure Coring Expedition Methods, *in* P. B. Flemings, S. C. Phillips, T. Collett, A. Cook, R. Boswell, and U.-G.-E. Scientists, eds., UT-GOM2-1 Hydrate Pressure Coring Expedition Report, Austin, TX, University of Texas Institute for Geophysics.
- Flemings, P. B., S. C. Phillips, T. Collett, A. Cook, R. Boswell, and U.-G.-E. Scientists, 2018c, UT-GOM2-1 Hydrate Pressure Coring Expedition Report, Austin, TX, University of Texas Institute for Geophysics.
- Liu, X., and P. B. Flemings, 2007, Dynamic multiphase flow model of hydrate formation in marine sediments: *Journal of Geophysical Research*, v. 112.
- Thomas, C., S. C. Phillips, P. B. Flemings, M. Santra, H. Hammon, T. S. Collett, A. Cook, T. Pettigrew, M. Mimitz, M. Holland, and P. Schultheiss, in press, Pressure-coring operations during the University of Texas Hydrate Pressure Coring Expedition, UT-GOM2-1, in Green Canyon Block 955, northern Gulf of Mexico: *American Association of Petroleum Geologist Bulletin*.

## ATTACHMENT B

### UT/DOE Ball Valve Actuation Testing Results



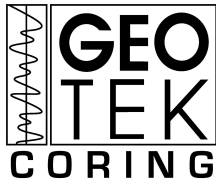
<b>UT/DOE Ball Valve Actuation Testing Results</b>	2020-10-01
--	------------

**Summary**

A group of isolated ball valve testing was performed with two different ball valve assemblies. The first ball valve assembly was the mark 4 version of the tool which is the same configuration that was used during CTTF 2020 testing. The second ball valve assembly used was the mark 5 version which includes an upgraded design to eliminate the jamming failures seen during CTTF 2020 testing. Each test included a water and grit solution with two different quantities of fine grit (53-125 µm particle size). The first quantity of grit uses 0.05 lbs of fine grit per 2.5 gallons of water. This ratio was identical to the 0.24% solids by weight extracted from the CTTF 2020 mud samples. The second quantity of grit used was 0.15 lbs of grit per 2.5 gallons of water, this quantity was used to evaluate how well the design modifications could perform in extreme conditions.

**Results**

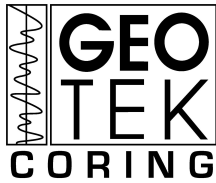
<b>9/29/2020 - Mark 4 Ball Valve Testing</b>			
<b>Test #</b>	<b>Test parameters</b>	<b>Test results</b>	<b>Video hyperlink</b>
1	Ball valve was actuated in a water and fine grit ( <b>53-125 µm</b> ) solution consisting of <b>0.05 lbs</b> of Aluminium Oxide per 2.5 gallons of water	<b>Failure</b> , ball valve closes approximately 50%	<a href="#">Mark 4 test 1</a>
2	Ball valve was actuated in a water and fine grit ( <b>53-125 µm</b> ) solution consisting of <b>0.05 lbs</b> of Aluminium Oxide per 2.5 gallons of water	<b>Failure</b> , ball valve closes approximately 75%	<a href="#">Mark 4 test 2</a>
3	Ball valve was actuated in a water and fine grit ( <b>53-125 µm</b> ) solution consisting of <b>0.05 lbs</b> of Aluminium Oxide per 2.5 gallons of water	<b>Failure</b> , ball valve closes approximately 25%	<a href="#">Mark 4 test 3</a>
4	Ball valve was actuated in a water and fine grit ( <b>53-125 µm</b> ) solution consisting of <b>0.05 lbs</b> of Aluminium Oxide per 2.5 gallons of water	<b>Failure</b> , ball valve closes approximately 75%	<a href="#">Mark 4 test 4</a>



\*All four tests with the Mark 4 ball valve assembly failed in the grit and water solution at a concentration of 0.05 lbs per 2.5 gallons of water.\*

<b>9/29/2020 - Mark 5 Ball Valve Testing (New seal batch)</b>			
<b>Test #</b>	<b>Test parameters</b>	<b>Test results</b>	<b>Video hyperlink</b>
1	Ball valve was actuated in a water and fine grit ( <b>53-125 µm</b> ) solution consisting of <b>0.05 lbs</b> of Aluminium Oxide per 2.5 gallons of water	<b>Failure</b> , ball valve closes approximately 60%	<a href="#">Mark 5 test 1</a>
2	Ball valve was actuated in a water and fine grit ( <b>53-125 µm</b> ) solution consisting of <b>0.05 lbs</b> of Aluminium Oxide per 2.5 gallons of water	<b>Pass</b> , ball valve fully closes, actuation was smooth with no interruptions	<a href="#">Mark 5 test 2</a>
3	Ball valve was actuated in a water and fine grit ( <b>53-125 µm</b> ) solution consisting of <b>0.05 lbs</b> of Aluminium Oxide per 2.5 gallons of water	<b>Pass</b> , ball valve fully closes, actuation was smooth with no interruptions	<a href="#">Mark 5 test 3</a>
4	Ball valve was actuated in a water and fine grit ( <b>53-125 µm</b> ) solution consisting of <b>0.05 lbs</b> of Aluminium Oxide per 2.5 gallons of water	<b>Failure</b> , ball valve closes approximately 90%, ball valve finished actuation after applying very little downward pressure on ball	<a href="#">Mark 5 test 4</a>
5	Ball valve was actuated in a water and fine grit ( <b>53-125 µm</b> ) solution consisting of <b>0.05 lbs</b> of Aluminium Oxide per 2.5 gallons of water	<b>Pass</b> , ball valve fully closes, actuation was smooth with no interruptions	<a href="#">Mark 5 test 5</a>
6	Ball valve was actuated in a water and fine grit ( <b>53-125 µm</b> ) solution consisting of <b>0.05 lbs</b> of Aluminium Oxide per 2.5 gallons of water	<b>Failure</b> , ball valve closes approximately 90%, ball valve finished actuation after applying very little downward pressure on ball	<a href="#">Mark 5 test 6</a>

\*Six tests were performed on the mark 5 ball valve assembly and 3/6 were successful. A new lot of manufactured seals were used in these six tests where we yielded lower results than previous testing,



further inspection on the new batch of seals revealed the the wiper rings to be tighter than the original batch of prototypes made\*

<b>9/30-2020 - Mark 5 Ball Valve Testing (Original seal batch)</b>			
<b>Test #</b>	<b>Test notes</b>	<b>Test results</b>	<b>Video hyperlink</b>
7	Ball valve was actuated in a water and fine grit ( <b>53-125 µm</b> ) solution consisting of <b>0.05 lbs</b> of Aluminium Oxide per 2.5 gallons of water	<b>Pass</b> , ball valve fully closes, actuation was smooth with no interruptions	<a href="#">Mark 5 test 7</a>
8	Ball valve was actuated in a water and fine grit ( <b>53-125 µm</b> ) solution consisting of <b>0.05 lbs</b> of Aluminium Oxide per 2.5 gallons of water	<b>Pass</b> , ball valve fully closes, actuation was smooth with no interruptions	<a href="#">Mark 5 test 8</a>
9	Ball valve was actuated in a water and fine grit ( <b>53-125 µm</b> ) solution consisting of <b>0.05 lbs</b> of Aluminium Oxide per 2.5 gallons of water	<b>Pass</b> , ball valve fully closes, actuation was smooth with no interruptions	<a href="#">Mark 5 test 9</a>
10	Ball valve was actuated in a water and fine grit ( <b>53-125 µm</b> ) solution consisting of <b>0.15 lbs</b> of Aluminium Oxide per 2.5 gallons of water. <b>This amount of grit is 3 times more than the previous tests</b>	<b>Pass</b> , ball valve fully closes, actuation was smooth with no interruptions	<a href="#">Mark 5 test 10</a>
11	Ball valve was actuated in a water and fine grit ( <b>53-125 µm</b> ) solution consisting of <b>0.15 lbs</b> of Aluminium Oxide per 2.5 gallons of water. <b>This amount of grit is 3 times more than the previous tests</b>	<b>Pass</b> , ball valve fully closes, actuation was smooth with no interruptions	<a href="#">Mark 5 test 11</a>
12	Ball valve was actuated in a water and fine grit ( <b>53-125 µm</b> ) solution consisting of <b>0.15 lbs</b> of Aluminium Oxide per 2.5 gallons of water. <b>This amount of grit is 3 times more than the previous tests</b>	<b>Failure</b> , ball valve closes approximately 90%, ball valve finished actuation after applying very little downward pressure on ball	<a href="#">Mark 5 test 12</a>
13	Ball valve was actuated in a water and fine grit ( <b>53-125 µm</b> ) solution consisting of <b>0.15 lbs</b> of Aluminium Oxide per 2.5 gallons of water. <b>This amount of grit is 3 times</b>	<b>Failure</b> , ball valve closes approximately 90%, ball valve finished actuation after lightly rattling	<a href="#">Mark 5 test 13</a>

	<b>more than the previous tests</b>	around in tube	
--	-------------------------------------	----------------	--

\*Seven more tests were performed on the Mark 5 ball valve assembly with the original lot of prototype seals that were manufactured. 6/7 of these tests passed, four of the seven tests were performed with three times the amount of grit used in the previous tests. 2/4 of these tests passed.\*

The final test performed was a pressure actuation test in the Geotek Coring down hole test facility. The test was performed with the mark 5 ball valve assembly at a bottom hole pressure of 3,000 Psi. The regulator on the pressure section was set to 4,479 Psi before deploying down hole. The purpose of this test was to validate that there are no issues during full down hole actuations with the new ball valve modifications. The test yielded successful results and the DST pressure plot can be seen below in figure 1.

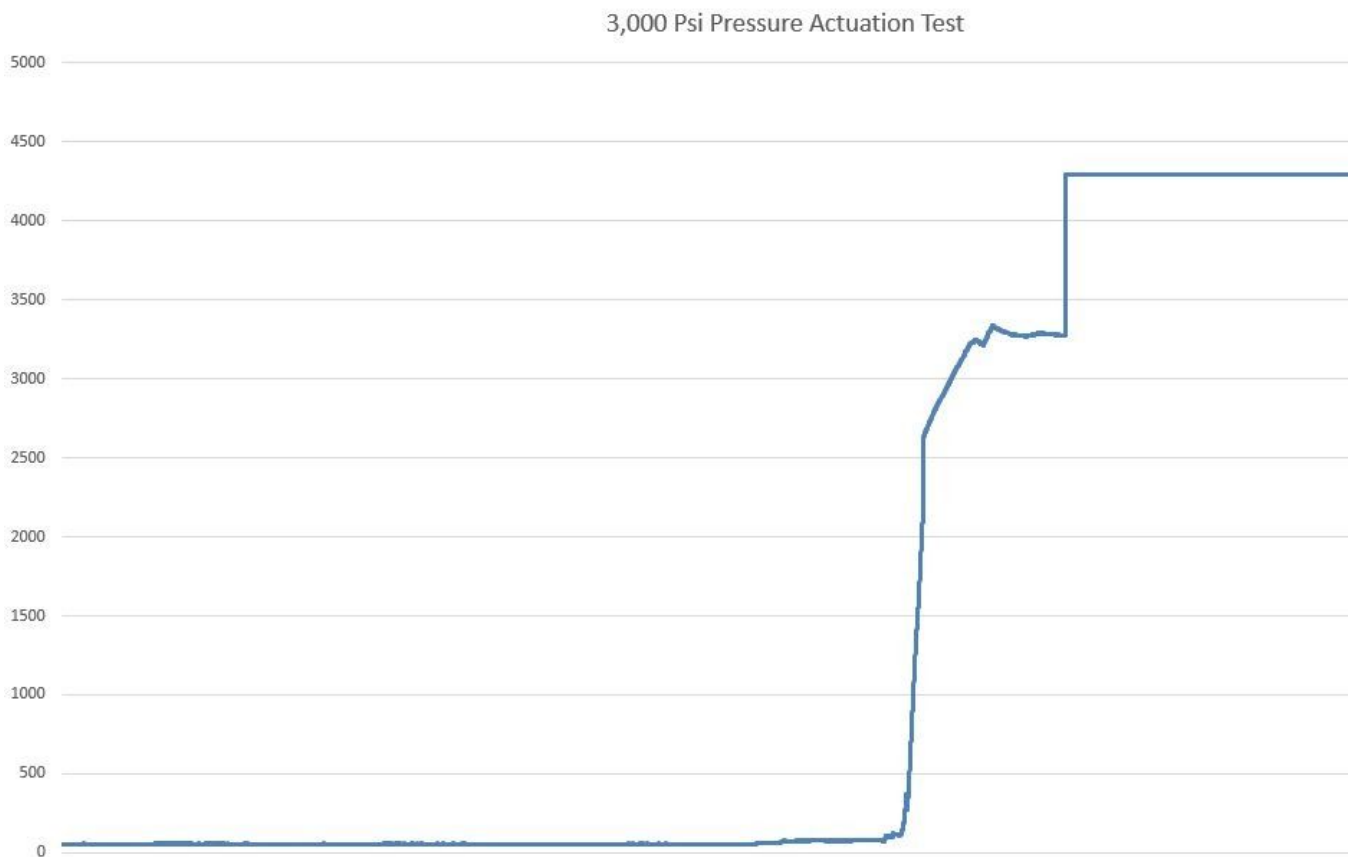


*Figure 1. DST pressure plot of pressure actuation test*

As seen above in figure 1, the tool successfully fires and registers a pressure boost from the pressure section. The tool was retrieved to the service unit and a final sealing pressure of 4,292 Psi was

recorded. This test validates that the mark 5 ball valve assembly does not change any timing or functionality of the tool in a down hole high pressure situation.

## Conclusion

During this round of testing we were able to successfully reproduce the ball valve jamming failures seen on the mark 4 ball valve assembly used during CTF 2020 testing. The mark 4 ball valve assembly **failed 4/4 tests** in a fine grit and water solution. Each of the mark 4 test failures were tested with a fine grit concentration of 0.05 lbs of grit per 2.5 gallons of water. This ratio is equivalent to the 0.24% solids by weight extracted from the CTF 2020 mud sample.

After demonstrating the failures of the mark 4 assembly, a group of testing was performed on the mark 5 upgraded ball valve assembly. The first six tests were performed in a solution with 0.05 lbs of fine grit per 2.5 gallons of water. This group yielded **3/6 passing tests**. These results were not consistent with the previous testing we had recorded and we determined that the only variable that was different was a newly manufactured batch of wiper rings. Upon closer inspection of the wiper ring seals, we confirmed that the new batch of wiper rings were dimensionally different and fit tighter onto the surfaces of the sliding components (Seal Carrier and Ball Follower). We then changed back to building the ball valve assembly with the originally manufactured batch of prototype wiper rings.

Three tests were performed on the mark 5 ball valve assembly after reverting back to the original batch of wiper ring seals. Each of these three tests included the 0.05 lbs of grit per 2.5 gallons of water solution. **3/3 tests passed** after changing the wiper rings.

In order to test the mark 5 assembly in more extreme conditions, four tests were performed with a fine grit concentration of 0.15 lbs of grit per 2.5 gallons of water. This concentration is equivalent to three times the amount of grit observed in the CTF 2020 mud sample. This group of testing yielded **2/4 passed tests**.

A quick evaluation of the mark 5 ball valve assembly after each failed test showed us that the ball valve would finish the stroke by applying a small amount of downward pressure. On one occasion, the ball valve finished the stroke after a failure by lightly rattling the assembly around in the tube.

Overall, the modifications from mark 4 to mark 5 improved the consistency of the ball valve when operating in conditions where fine grit particles are present. In order to be fully confident in returning the tool to test in CTF we plan to continue with tuning the design until it can pass in extreme grit conditions 100% of the time. The design adjustments we plan to make to further improve the tool include the following:

- Refine seal tolerancing and improve quality control for wiper rings on Seal Carrier and Ball Follower
- Modify ball follower design to eliminate fluid compensation ports where grit builds up